Journal of Environmental Science Studies; Vol. 8, No. 2, 2025
ISSN 2591-779X E-ISSN 2630-4821
Published by July Press

Application of Consecutively Assembled Boulders Around Hydraulic Structures

Youichi Yasuda[1]

[1] Department of Civil Engineering, College of Science and Technology, Nihon University, Tokyo, Japan

Correspondence: Prof. Youichi Yasuda, Civil Engineering Dept., College of Science and Technology, Nihon University, Tower Schola S1010, 1-8-14 Kanda Surugadai, Chiyoda-ku, 101-8308 Tokyo, Japan. E-mail: yasuda.youichi@nihon-u.ac.jp

Received: September 30, 2025 Accepted: October 27, 2025 Online Published: December 3, 2025

doi:10.20849/jess.v8i2.1537 URL: https://doi.org/10.20849/jess.v8i2.1537

Abstract

The riverbed protection below hydraulic structures must require from the viewpoint of preservation of river environment. In the case of bridge pier, a deflected flow due to impingement to the front of pier makes water surface slope and undulation flows with stable and irregular form downstream of the pier. It is important to pay attention to the effects of irregular undulating flows on riverbeds, as even if the average flow velocity near the bottom is low, their ability to promote irregular transport of sand and gravel is not negligible. For the movable weir, if the river is wide, there will be multiple gates, and the flow deflected by impinging the gate pier with the support will form a flow like that of the bridge pier, and the undulations with stable wave and irregular wave will cause riverbed erosion over a long period of time. For the energy dissipator downstream of the low drop structures, jump formation is useful, but a concave curvature at the toe of the jump does not neglect, and the mainstream is located near the bed. The riverbed protection needs downstream of jump region. Recently, the author discovered that the installation of consecutively assembled boulders is effective in reducing the flow velocity near the bottom, and in controlling the mainstream during normal and flood stages. The ramp with the consecutively assembled boulders was constructed according to the author's proposal, the upstream and downstream migration for muti-aquatic animals in normal stages was confirmed in prototype. In this paper, to prevent local scouring occurring at the downstream of movable weirs, low-drop structures, check dams, and around bridge piers, the author experimentally demonstrated a riverbed protection method using seepage flow by placing crushed stone downstream of consecutively assembled boulders arranged in a parabolic shape. The experimental results revealed that the combination of assembled boulders installation and protection region with crushed stones makes effective application of the formation of seepage flow and supporting by the velocity field near the bottom. Further, the application of the consecutively assembled boulders in prototype was introduced, and the proposed structure might help ecological approach.

Keywords: assembled boulders, riverbed protection, seepage flow, ecological approach, local flow

1. Introduction

Hydraulic structures such as dams, weirs, check dams, and bridge piers are installed across rivers for purposes such as water supply, power generation, flood control, sediment control, and traffic transportation. According to the hydraulic engineering design manual (e.g., Engineering Manuals & Monographs 2022, The Collection of Hydraulic Formulae 2019, Japan River Association., 2005), riverbed protection methods were specified. However, in fields, local scouring, riverbed degradation, and structural damage occur during floods. It is considered that a method for attenuating flow velocity near the bottom surface has not yet been established. While there are methods to forcibly raise the main flow toward the water surface, the main flow re-positions itself near the bottom surface downstream, leading to localized scouring.

For local scouring around bridge piers, countermeasures are sometimes taken to protect the riverbed from the bottom flow velocity near the bridge piers (Umeda et al. 2010, Vijayasree 2019, Chiew 2002, Takashi, et. al. 2021, and Zhang, 2022). Study on local scour protection countermeasures of bridge pier. Highlights in Science, Engineering and Technology,). However, there are no methods to control the flow that is deflected by colliding with the bridge piers, resulting in scouring (Ettema et al., 2006).

To control water levels during flood stages at the upstream of weir, concrete weirs as low head drop structure have been changed to movable weirs (Japan River Association., 2005). In the case of movable weirs, as the gates are completely opened during flood stages, a hydraulic jump is not formed. The passing through the weir is

subcritical flow during flood stages. In this case, the approaching flow impinges on the support piers guiding the gates, and a deflected flow is formed. The mainstream position in the deflected flow is located near the bottom. At the downstream of the concrete apron of the weir, the protection blocks are installed but riverbed scouring occurs (Breusers and Raudkivi 1991).

For dams with spillways, the energy dissipation device is mandatory. It is particularly important to control the downstream water level required to form hydraulic jump in stilling basin by installing a sub-dam. As the river protection method downstream of the sub-dam, the concrete apron and protection blocks were installed. But local scouring may still occur in the case of low head drop structures (Yasuda and Shinozaki 2018).

In the case of check dams, the main purpose is to control debris flows and sediment transport, and the energy dissipation basins are installed. However, there is little emphasis on controlling the flow downstream of the energy dissipation basins (Yasuda and Wang 2024). During flood stages, instantaneous transport leads to erosion and riverbed lowering. Further, as sediment control improvement plans progress, sediment production restricted, and riverbed lowering progressed due to local scouring.

Recently, the author discovered that the installation of consecutively assembled boulders may be useful in mitigating local scouring downstream of slit-type check dams, movable weirs, low-head structures, and bridge piers (Yasuda and Wang 2024, Yasuda and Suzuki 2023, Yasuda and Ishitsuka 2023, Yasuda and Fuchino 2022). In other studies (Pagliara et al. 2008, 2015, and 2017, Kim 2017, Chaudhary 2021, Takashi et al. 2021), the installation of boulders was applied for the rump, roughness bed. In these cases, the boulders were fixed by concrete because of inadequate techniques for stabilizing large boulders during flood stages. Alternatively, excessively large boulders were installed. The installation of the consecutively assembled boulders without binding materials (see Figure 1) remains stable even during floods. Further, the structure of consecutively assembled boulders makes the seepage flow formation, and the seepage flow may help the velocity reduction near the bed (Yasuda 2025). In these experiments, local scouring easily occurs at the downstream end of assembled boulders because there is no transition zone between the assembled rock blocks with an average size of 9.5 cm and the pebbles with an average size of 5.3 mm. As a result, in the flow passing through the top of assembled boulders, the flow velocity near the bed decays. The formation of seepage flow between crushed stones may help the reduction of the velocity near the bed. Experiments with scale models conducted under Froude similarity, and the results might apply to the prototype. It is important how the seepage flow velocity measured in the experimental model applies to the prototype because the porosity ratio inside boulders may depend on the scale of boulders.

This paper presents the improvement method for countermeasure against local scouring at the downstream of hydraulic structures, i.e., low drop structure, slit-type check dam, bridge piers, and movable weir. The measurement of the velocity distributions including turbulent intensity evaluated the mainstream position at the downstream of the hydraulic structures under the Froude similarity. Experiments have shown that the transition zone from boulders to crushed stones contributes to the reduction of flow velocity near the bottom, and that the combination between parabolic installation of consecutively assembled boulders and protection area due to crushed stones may help mitigate flow velocity due to deflected flow caused by structural passage. Regarding the interaction between flow velocity near the bed surface and seepage velocity, the application of the proposed structure is the most important, and actual example supported the experimental results on the flow velocity distribution and magnitude. Furthermore, the proposed structure using consecutively assembled boulders in prototype (e.g., ramps, around bridge piers) was beneficial to the natural environment by enabling the upstream and downstream migration of aquatic animals, balancing flood control and riverine environmental considerations.

2. Experimental Setup

This study was experimental investigation on abrupt drop structure, ramp with assembled boulders, slit-type check dam, bridge pier, and movable weir with a support pillar (Figure 1). Experiments were conducted by installing physical models on a horizontal rectangular channel 15 m long, 0.8 m wide, and 0.6 m height. In the protection region against local scouring, the consecutively assembled boulders were installed. If the size of the boulder is defined as the average length of the long side, short side, and height (Yasuda and Umemura 2023), the average size of the boulder was 0.092 m (porosity ratio 50%). To estimate the spatial volume of deposited gravels, the weight of water (W_w) was measured using a plastic container, and the water level within the container was recorded. Gravels were then inserted into the container up to the recorded water level, and the water was added to the water level. After removing the gravel, the weight of the water (W_{wb}) was measured, and the porosity ratio (W_{wb}/W_w) was calculated. When constructing assembled boulders, the boulders are in a staggered pattern, and the boulders on the downstream side are tilted so that the load is transmitted to them, and there are at least four contact points between the boulders in vertical and horizontal directions as well as at the bottom (Figure 2). On the downstream side, crushed stones with an average size of 0.016 m (porosity ratio 41 %) were installed. In the case of two experiments for bridge pier and movable weir, as shown in Figure 1 (a and d),

pebbles stones with an average size of 0.0053 m (porosity ratio 32 %) installed. The water surface profile, bottom profile and flow velocity measured at a model discharge, assuming a flood stage. The downstream water level controlled by using a lifting sluice gate located at channel end section. For the measurement of the water surface profile and bottom profile, using a point gauge, and a 2D electromagnetic current meter (measurement time: 30 sec, measurement interval: 0.05 sec) with a KENEK-made I-type probe was useful for the measurement of flow velocity (https://www.kenek-co.com/english/index.html). For areas that were difficult to measure using the electromagnetic current meter, a KENEK-made propeller-type current meter (measurement time: 20 sec) was helpful. The flow velocity within the seepage flow measured in a space created by embedding a circular coil with an inner diameter of 2 cm coated with enamel in gravels in advance.

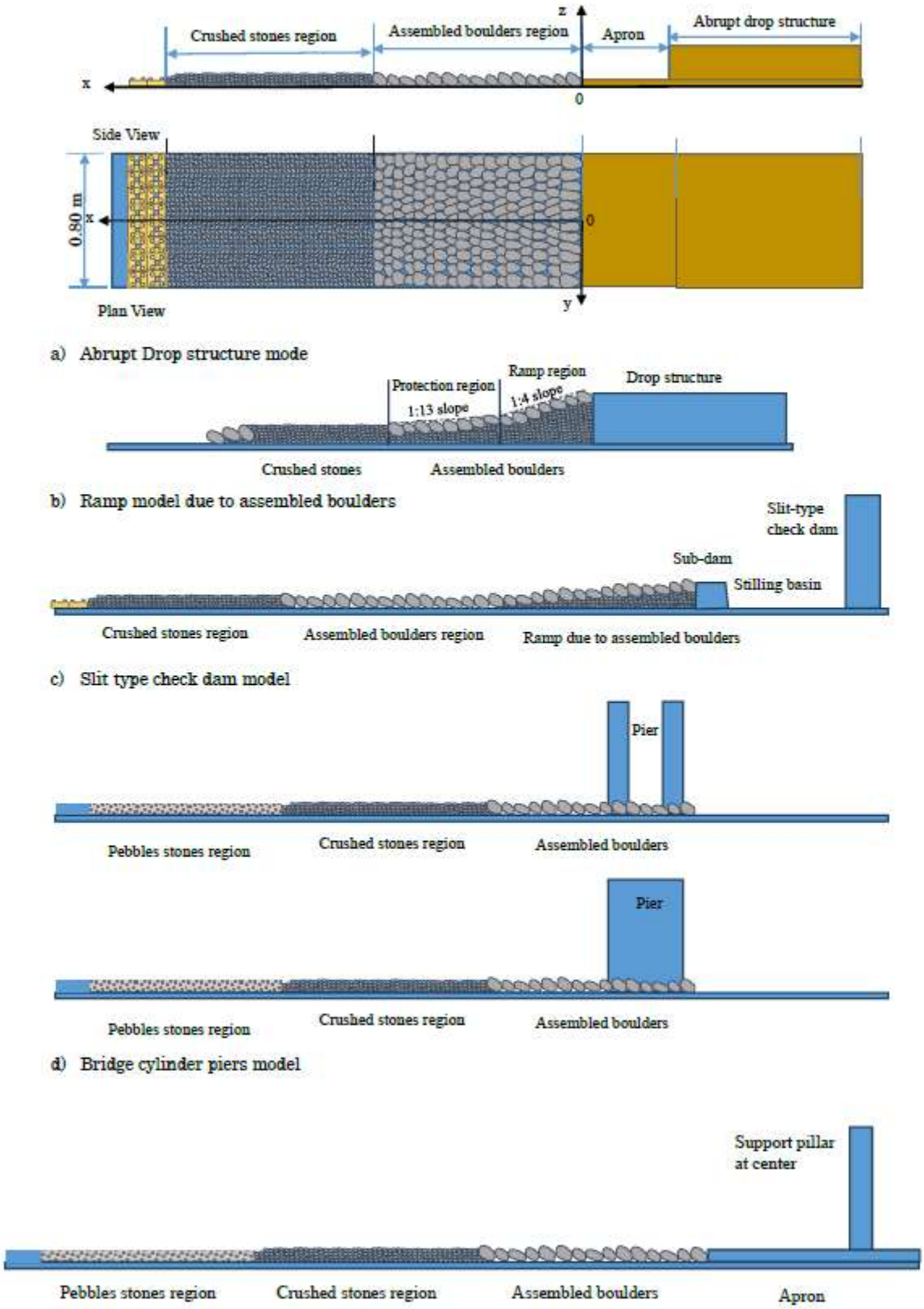

e) Movable weir model

Figure 1. Installation of assembled boulders and crushed stones in physical models

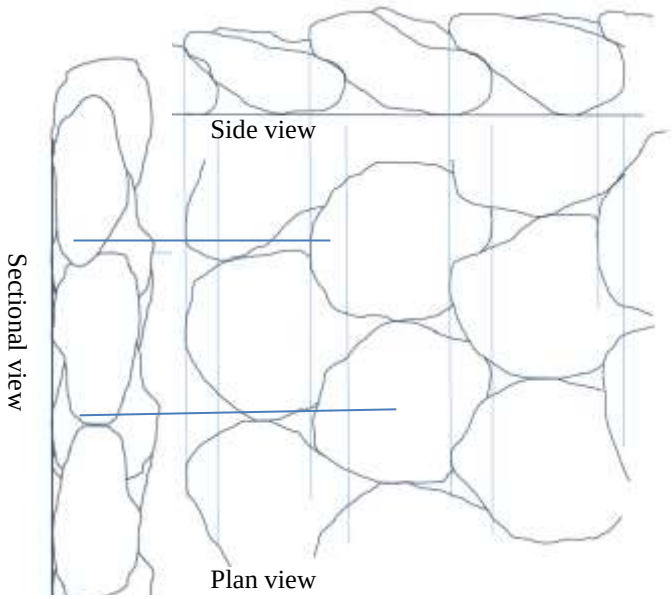

Figure 2. Structure of Consecutively Assembled Boulders in Physical Model

3. Movable Wier with Support Pillar

The installation of the consecutively assembled boulders shown in Figure 3 (a) is effective for the protection against the local scouring downstream of the movable weir during flood stages (Yasuda and Suzuki 2023). Flood flows passing over the movable weir include the formation of deflected flows affected by collisions with support pillar. The assembled boulders may be useful for lifting the main flow and for reducing the flow velocity near the bottom due to seepage flow. Three-dimensional flow structures caused by deflected flows remain downstream of the assembled boulders, and the time-average flow velocity accelerate by the deflected flows. For an extended period during floods, it might be difficult to protect the bottom under the installation of the assembled boulders only, a local scouring might be formed. Then, crushed stones are installed as protection region (Figure 3 (b)), and the formation of the seepage flow inside crushed stones is effective for the reduction of the flow velocity near the bottom which may help the protection against the local scouring for a long period. Figure 4 shows flow condition passing through a movable weir with support pillar of gates during a flood stage. The discharge was set as a maximum discharge supplied in environmental hydraulic laboratory of Nihon university (0.150 m^3/s). In the installation region of the assembled boulders, a stable undulation surface formed. On the other hand, undulation is unstable in the protection region with crushed stones. Furthermore, a deflected flow formed downstream due to collision with the support pilar (Figure 5). To mitigate a three-dimensional fluid structure due to the deflected flow and cause the main flow to rise toward the water surface, the consecutively assembled boulders installed nearly horizontally in X direction (Figure 6) and parabolically in the transverse direction (Figure 7). Figure 6 shows the water surface and bottom profiles under a maximum discharge. When the protection area is determined to be the optimal installation length of crushed stones (L = 140 cm), local scouring does not occur even downstream of the crushed stones. As shown in Figure 9 (a), when the installation length of the crushed stones is set to L = 70 cm, localized erosion forms after 70 hours from the start of the experiment. However, when the installation length is set to L = 140 cm, no erosion occurs even after the same duration (Figure 9 (b)).

(a) Plan view of assembled boulders (b) View from pebbles to assembled boulders

Figure 3. Installation of assembled boulders, crushed boulders, and small pebbles downstream of weir

(a) Flow condition on crushed stones and pebbles (b) Flow condition on assembled boulders and apron

Figure 4. Flow condition passing through movable weir with support pier of gates during a flood stage

Figure 5. Deflected flows downstream of support pier

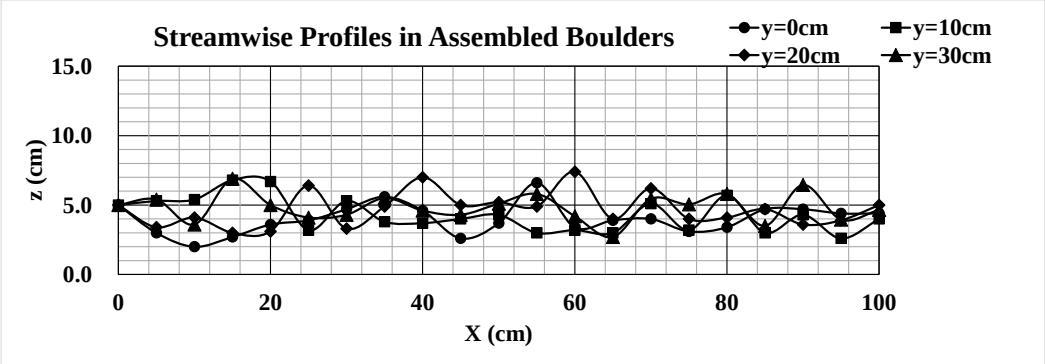

Figure 6. Streamwise change of bottom surfaces in the installation region of assembled boulders

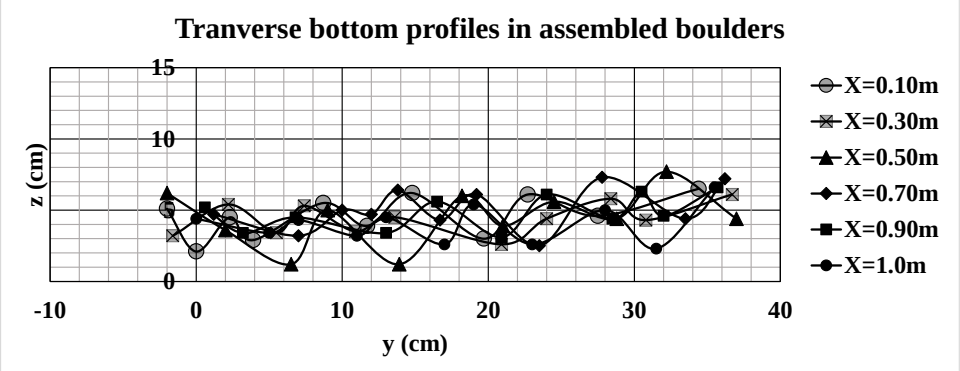

Figure 7. Transverse change of bottom surfaces in the installation region of assembled boulders

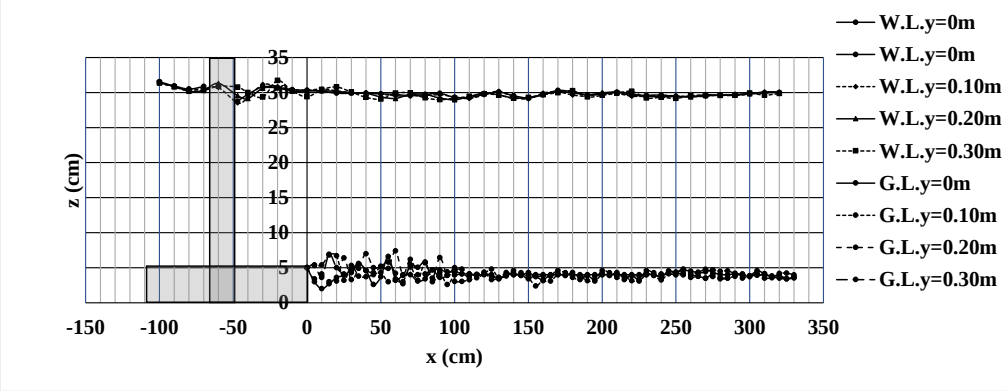

Figure 8. Water surface and bottom profiles

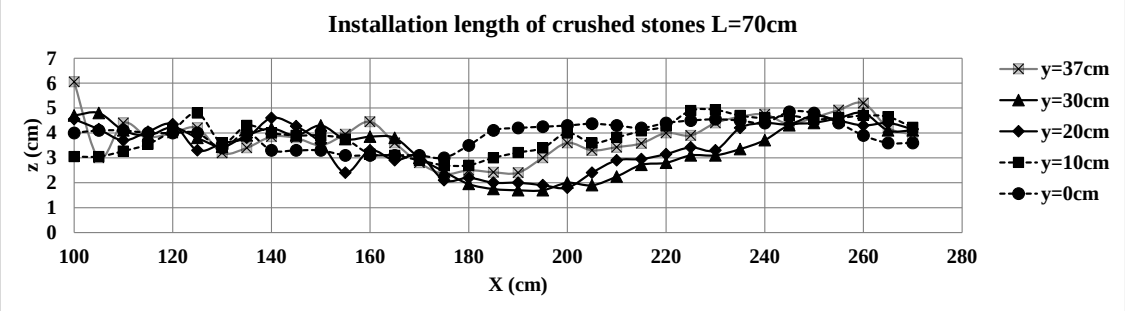

(a) L = 0.70 m

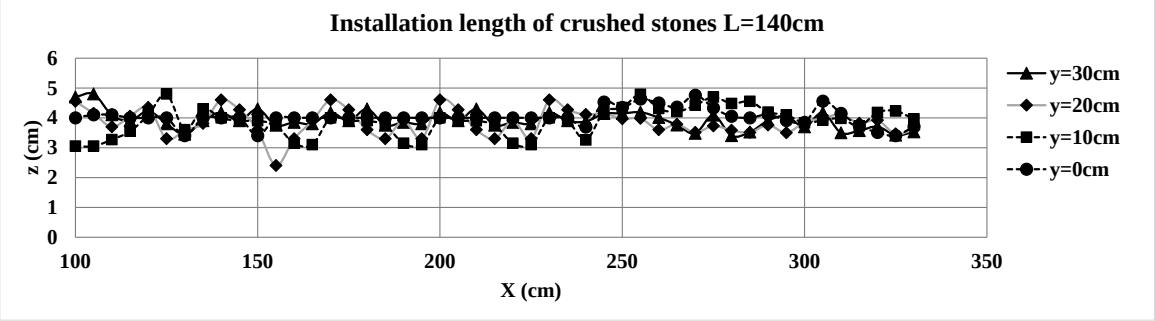

(b) L = 1.40 m

Figure 9. Bottom surface profiles (y = 0 m, 0.10 m, 0.20 m, 0.30 m, and 0.37 m)

Figure 10 shows streamwise change of maximum velocity at y = 0 m, 0.10 m, 0.20 m, and 0.30 m. As the support pilar is in the center part of channel, the maximum velocity at y = 0 m is always smaller than that at y = 0.30 m. The maximum flow velocity increased from the center toward the side walls due to the influence of the deflected flow that collided with the support pillars, and there was almost no decay of the maximum flow velocity at the downstream of the assembled boulders (X > 100 cm). Regarding the standard deviation for X component, as shown in Figure 11, the streamwise change is small, and u' is almost 8 to 10 cm/s. The position of the maximum flow velocity downstream of the assembled boulders at y = 0.20 and 0.30 m is always lower than that at y = 0 and 0.10 m due to the formation of a three-dimensional flow structure caused by deflection flow (Figure 12). From this point, the reduction of the flow velocity near the bottom is necessary in the installation region due to crushed stones.

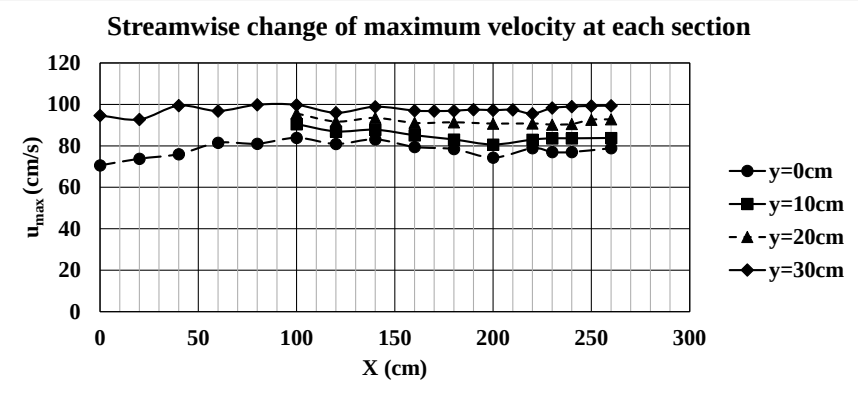

Figure 10. Streamwise change of maximum velocity at y = 0 m, 0.10 m, 0.20 m, and 0.30 m

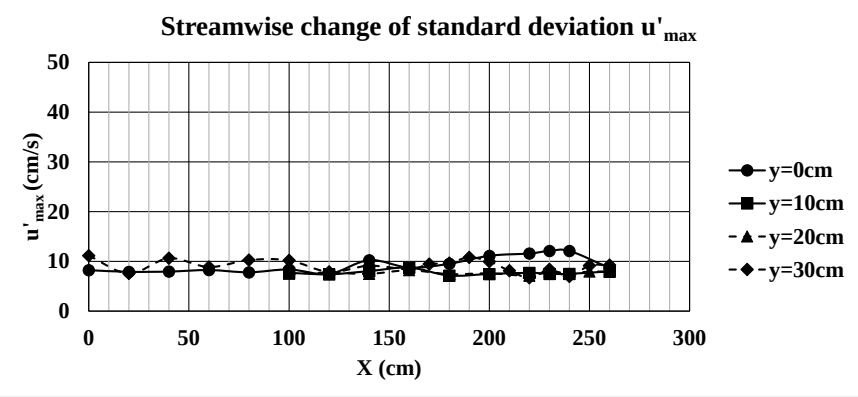

Figure 11. Streamwise change of standard deviation of maximum velocity at y = 0 m, 0.10 m, 0.20 m, and 0.30 m

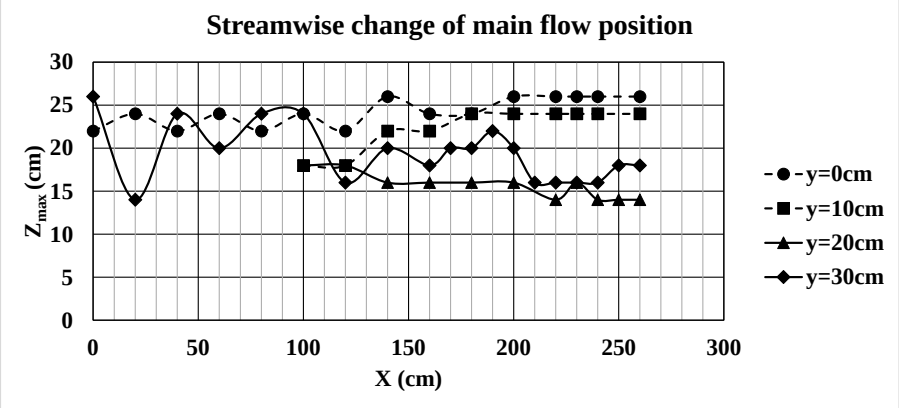

Figure 12. Streamwise change of position of maximum velocity

Downstream of the assembled boulders, the velocity profiles at y = 0 and 0.1 m differ from those at y = 0.2 and 0.3 m (Figure 13). Additionally, due to the effective reduction in flow velocity caused by seepage flow near the bottom, the flow velocity near the bottom at y = 0.2 m and 0.3 m decreases to a level where scouring does not occur, even if influenced by the flow velocity distribution caused by deflected flow. As shown in Figure 14, the main flow in subcritical flow is located near the side within the range of $1.0 \leq X/La \leq 2.6$, and a three-dimensional structure due to the deflected flow continues far downstream under the installations of the assembled boulders and crushed stones. The installation region of crushed stones to reduce the concentration of the main flow due to the deflected flow is required.

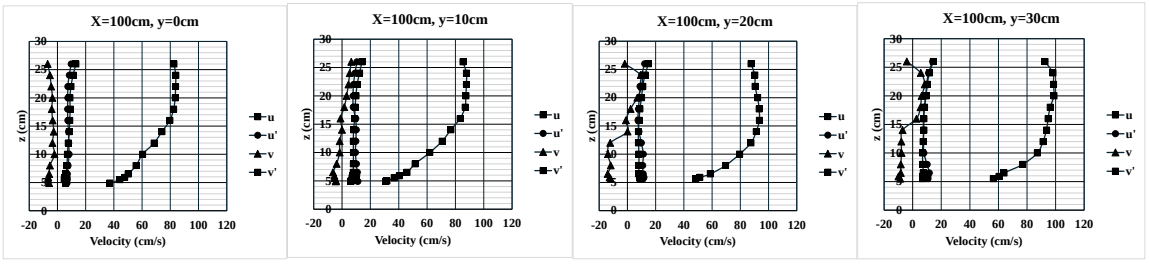

(a) X/La = La/La = 1.00

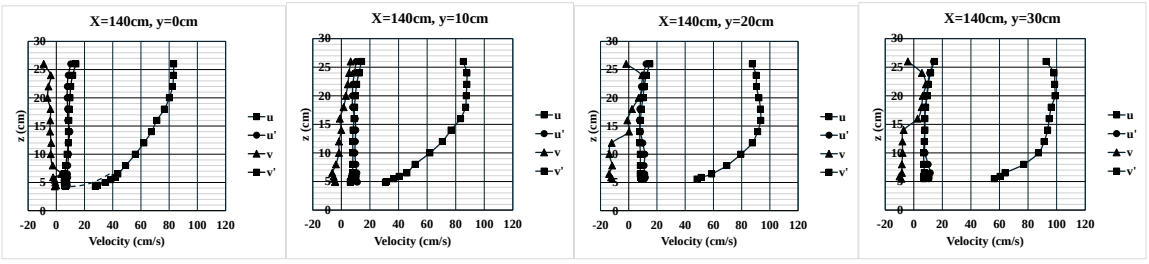

(b) X = (La + Lp -1.0)/La = 1.40

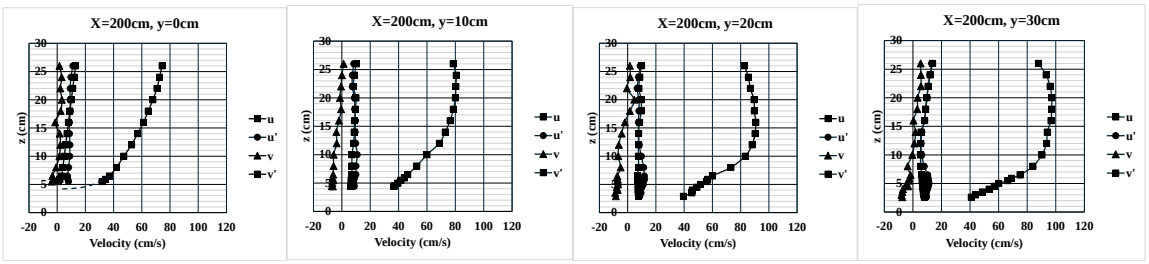

(c) X/La = (La + Lp - 0.6)/La = 2.00

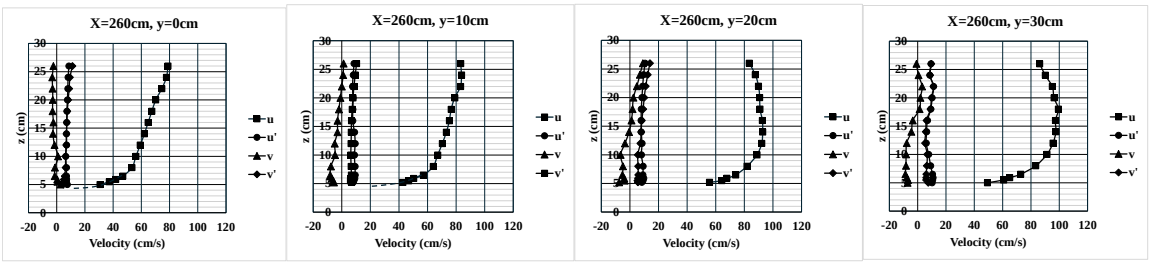

d) X/La = (La + Lp + 0.2)/La = 2.60

Figure 13. Velocity profiles at each section (y = 0, 10, 20, and 30 cm)

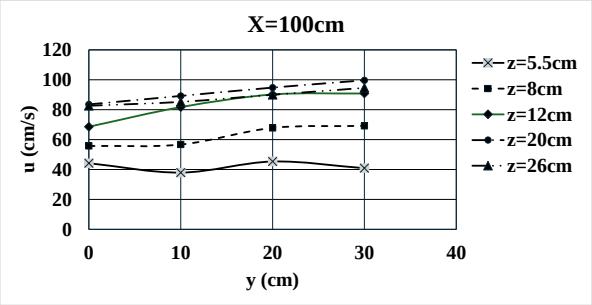

(a) X/La = 1.00

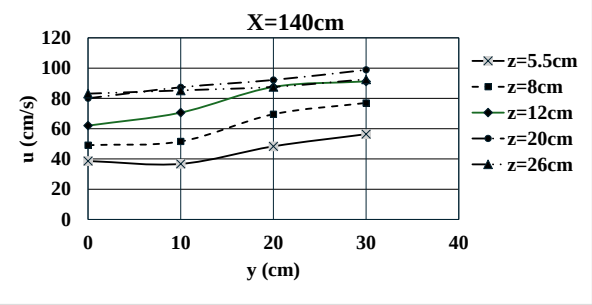

(b) X/La = (La + Lp -0.6)/La = 1.40

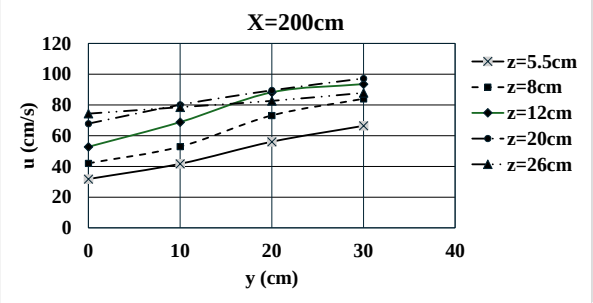

(c) X/La = (La+Lp-0.4)/La = 2.00

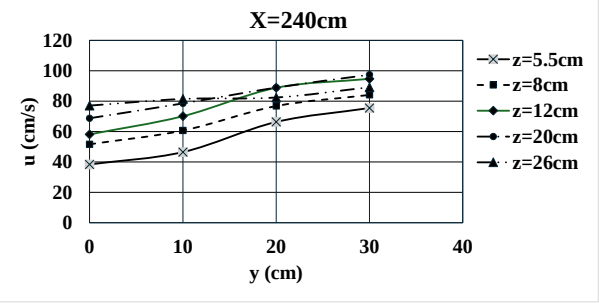

(d) X/La = (La+Lp)/La = 2.40

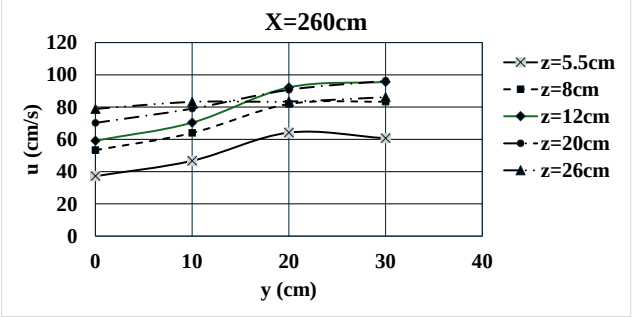

(e) X/La = (La+Lp+0.2)/La = 2.60

Figure 14. Transverse change of time averaged velocity at same vertical position

4. Abrupt Drop Structure

In the low drop structure, the apron and the protection region are installed in accordance with the hydraulic design manual. As an energy dissipater below the low drop, the formation of hydraulic jump with a surface roller is general (Hager 1992). If a concave curvature of the streamline at the toe of jump is large in the jump formation below the low drop structure, the main flow in the jump is located near the bottom (Yasuda and Shinozaki 2018, 2019, Liu et al. 2004). Also, the deflected flow forms at both sides downstream of the jump, and the flow velocity in the deflected flow is higher than that at the center part of the jump. As the installation of protection blocks may not help with the protection against local scouring at the downstream of the protection region (Farhoudi and Smith 1985), the consecutively assembled boulders instead of bed protection blocks are applicable in the protection region (Figure 15). The measurements of the water surface profile, riverbed profile and flow velocity were taken at a model discharge of Q = 0.150 m^3/s, assuming a flood stage. The tailwater level is controlled in order that the toe position of the jump is located at $x \approx 0$ by using a lifting sluice gate located at channel end section.

Figure 15. Physical model for both low drop structure and protection region due to assembled boulders

Figure 16 shows water surface profiles of the jump with a surface roller just below a low drop and the bottom profiles of the assembled boulders and crushed stones. The tops of the boulders in the assembled boulders arrangement area gradually rise toward the downstream direction, forming a mainstream inside the jump that rises toward the water surface. Figure 17 shows the flow condition of the jump formation. As shown in Figure 17, the installation of the consecutively assembled boulders in the protection region is effective for raising the main flow toward water surface. The air entrainment region moves from the bottom toward the water surface in the jump formation formed on the assembled boulders. A seepage flow makes a low velocity inside boulders, and the velocity near the bottom might be reduced.

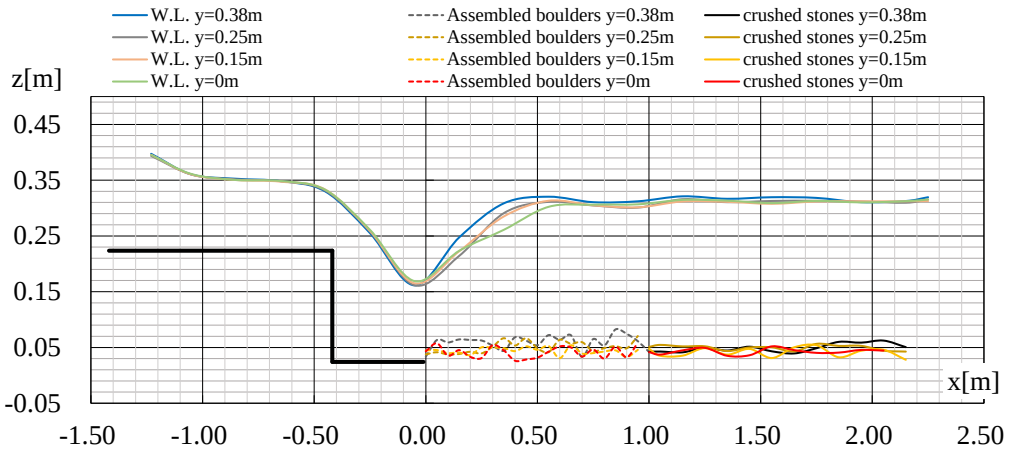

Figure 16. Water surface and bottom profiles

Figure 17. Flow condition downstream of low drop structure

The main flow paths are defined by the locations of the maximum time-average flow velocities evaluated in each vertical cross-section. As shown in Figures 18 and 19, the maximum flow velocity, including its standard deviation (i.e., turbulent intensity), decays within the protected area. The transverse difference of the maximum velocity decays is small. Additionally, the deflected flow caused by the flow passing through an abrupt drop structure impinging on the bottom surface directed toward the center of the channel by arranging the assembled rock blocks in a parabolic shape, resulting in a slight decrease in the maximum flow velocity at y=0.38 m. The position of the maximum time-average flow velocity in the jump region rises toward the water surface (Figure 20).

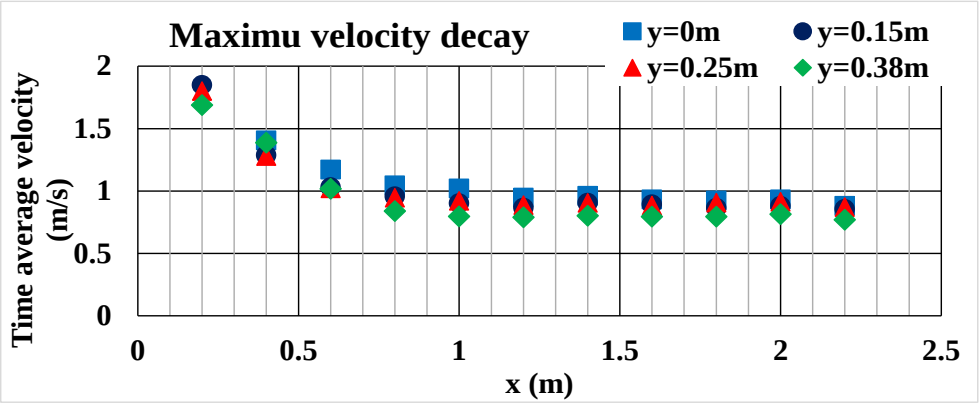

Figure 18. Maximum time average velocity decays

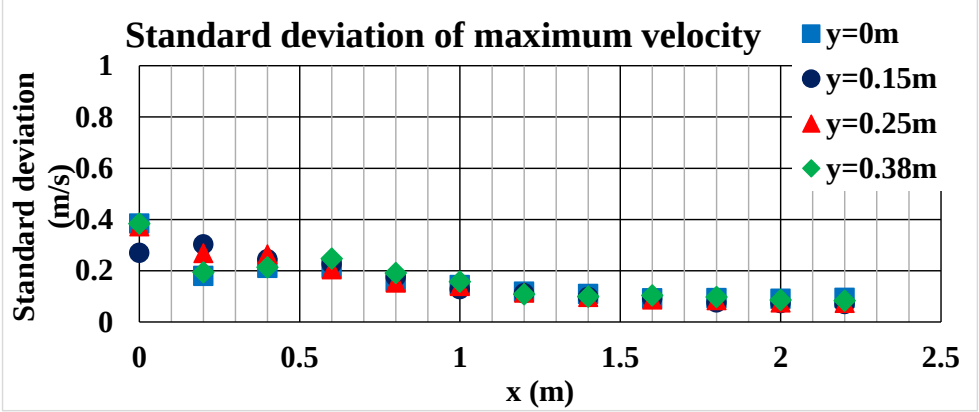

Figure 19. Streamwise change of standard deviation of maximum velocity

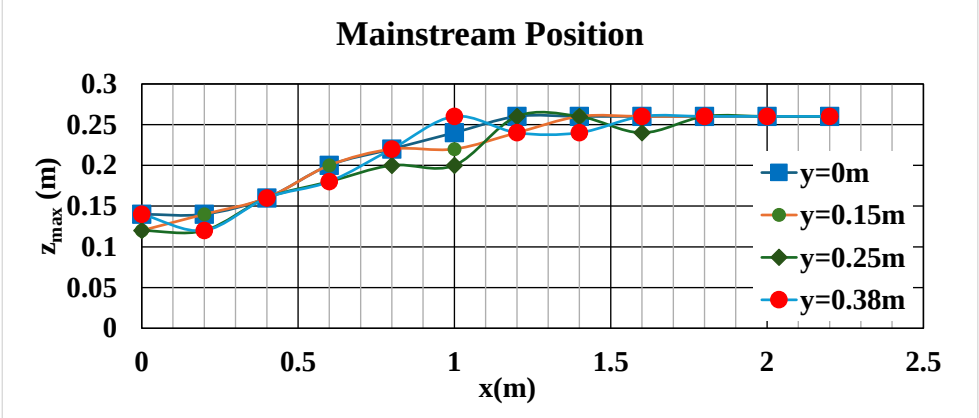

Figure 20. Streamwise change of position of maximum velocity at each vertical section

Furthermore, as shown in Figure 21, the velocity near the bottom surface decreases even 0.009 m (the height at which the flow velocity measured when the probe touches the bottom surface) above the bottom. Because crushed stones installed downstream of the assembled boulders as a protection zone, and the standard deviation of velocity (i.e., turbulence intensity) near the bottom surface reduced by seepage flow inside the crushed stones (Figure 22).

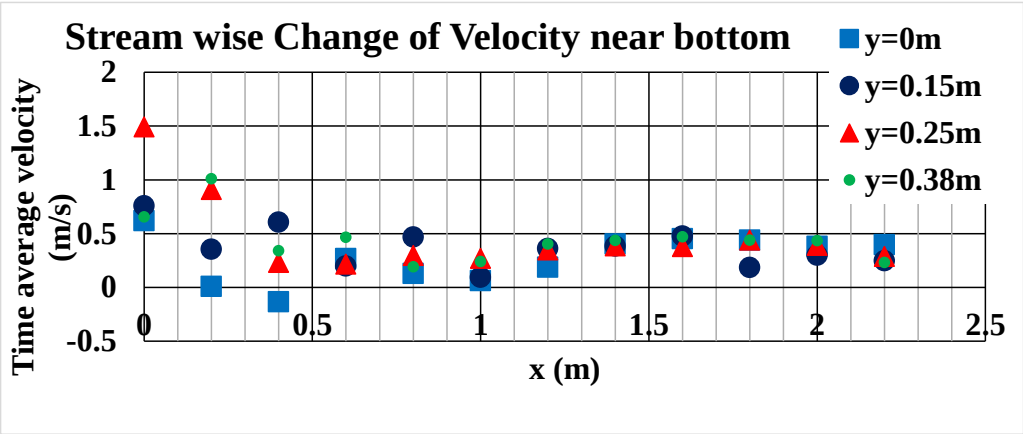

Figure 21. Streamwise change of time average velocity near bottom

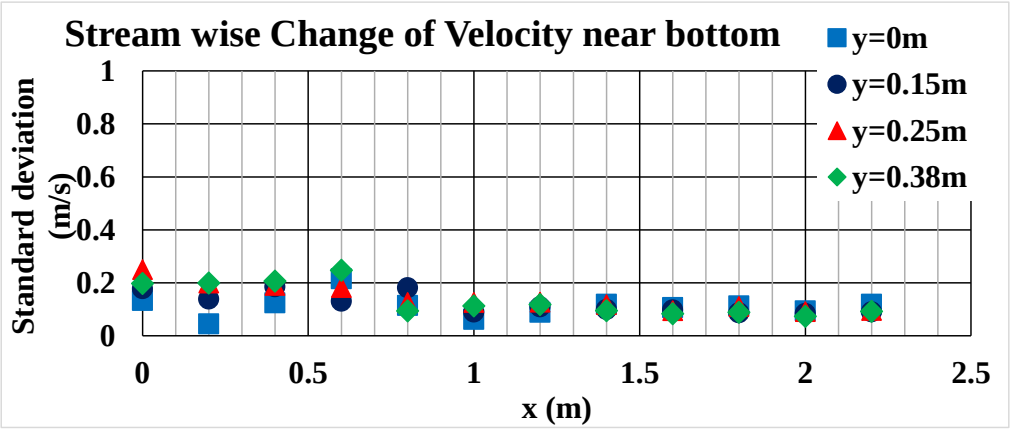

Figure 22. Streamwise change of standard deviation of flow velocity near bottom

Figure 23 shows velocity profiles including standard deviation (i.e., turbulent intensity) at x = 0.40 m, 0.60 m, 1.0 m, and 1.80 m. Then, u and v are time average flow velocity for x and y components, respectively. u' and v' are standard deviation for x and y components, respectively. In the installation region of assembled boulders, the propeller velocity meter enabled the measurement of time average flow velocity u if the velocity measurement due to electrical magnetic velocity meter is impossible by the air-entrainment. The flow near the side wall has less bubble entrainment, and not only the time average but also the standard deviation can evaluate up to z = 0.25 m. Furthermore, even in the jump region, the velocity gradient near the bottom surface is small, and the turbulence intensity does not increase in the downward vertical direction. This might explain that the velocity of the seepage flow influences the velocity near the bottom. At the end of the jump (x = 1.00 m), the time-average flow velocity of x-component shows different distributions between y = 0 m and y = 0.38 m due to the deflected flow controlled by the parabolic shape of assembled boulders. The standard deviations for both x and y components decrease in the downward vertical direction. In the installation region of crushed stones, the standard deviations for both x and y components are almost constant in the z direction. The deflection caused by the assembled boulders affects the time-averaged flow velocity and shows different distributions between y = 0 m and y = 0.38 m.

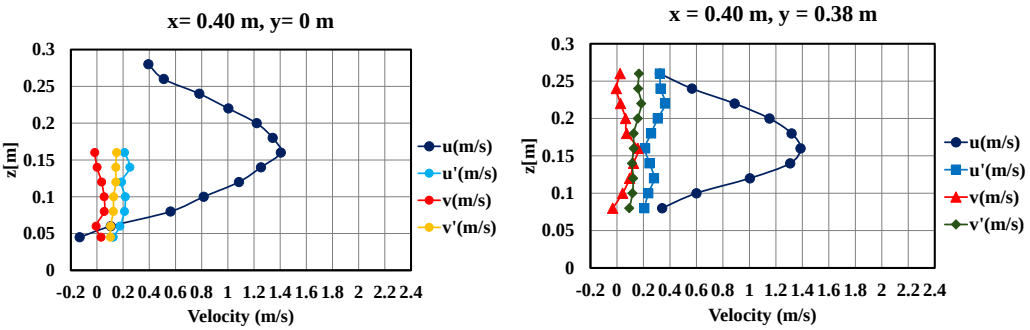

a) x =0.40 m (middle part of assembled boulders installation)

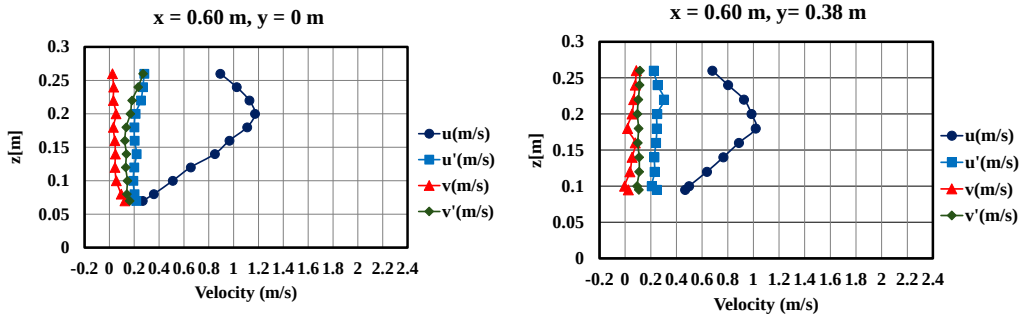

b) x =0.60 m (middle part of assembled boulders installation

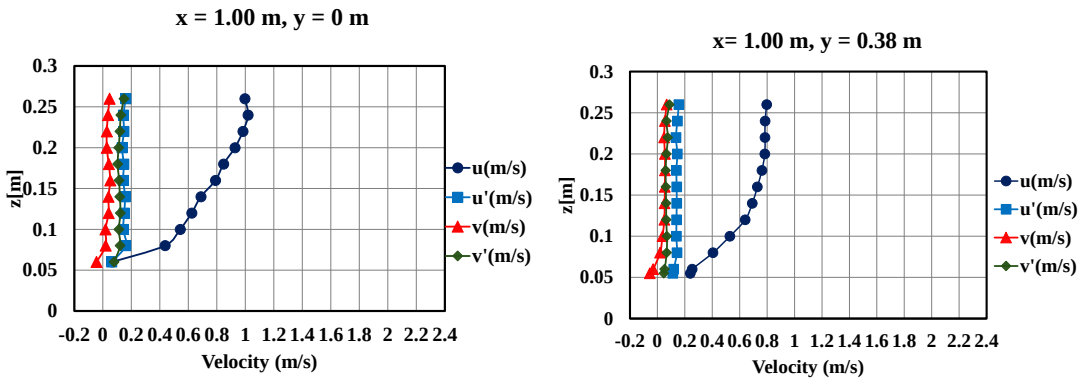

c) x =1.00 m (downstream end of assembled boulders installation)

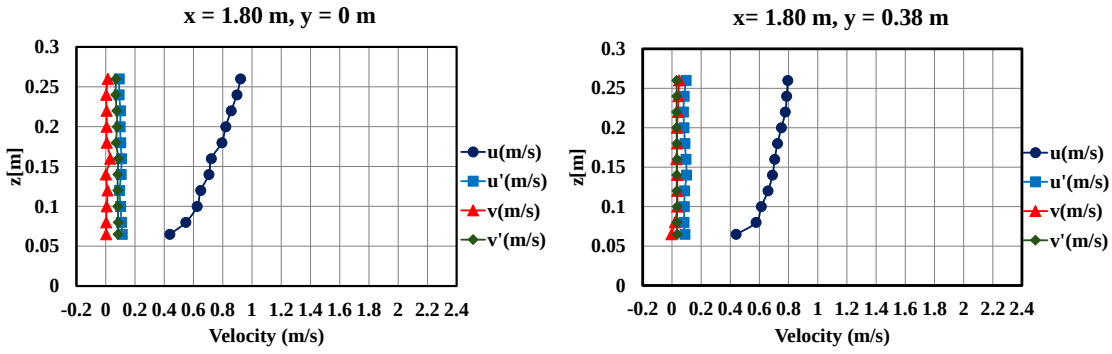

d) x =1.80 m (crushed stones region)

Figure 23. Velocity profiles at each vertical section

5. Ramp Due to Assembled Boulders

Drop structures obstacle the upstream and downstream migrations of aquatic animals. Even if concrete blocks are installed for riverbed protection during floods, local scouring easily occurs downstream of drop structures. Damage to structures is severe in areas where debris flows, driftwood, and boulders transport during flood stages. Further, there is a scouring hole downstream of the concrete apron or stilling basin for a long time by the impingement of flooding flow passing over drop (Breusers, H. N. C. & Raudkivi, A. J. 1991). During normal stage, drop structure causes the formation of drowning machine, generates unpleasant running water noise due to low-frequency vibrations, not only inhibits the migration of aquatic animals. Then, as shown in Figure 24, the author proposed the installation of ramps with consecutively assembled boulders across the entire drop section to reduce the velocities near the bottom in a high velocity flow passing over drop structure (Yasuda and Fuchino 2021). Further, for the velocity reduction downstream of assembled boulders, crushed stones are installed as a transition zone. Figure 25 shows bottom profiles in assembled boulders and crushed stones regions. The installation shape of the assembled boulders is parabolic to deflect the main flow toward the center part.

(a) View point from downstream part (b) Bird view

Figure 24. Construction of assembled boulders

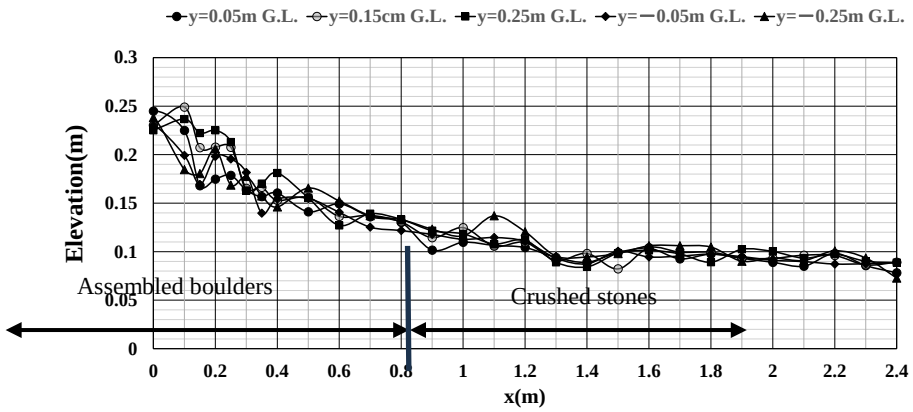

Figure 25. Bottom profiles in assembled boulders and crushed stones regions

Figure 26 shows flow condition during a flood stage (maximum discharge Q = 0.150 m^3/s in experimental channel). As the ramp is composed of the installation of consecutively assembled boulders, a high velocity flow near the bottom may reduce by a low velocity of seepage flow inside boulders. In a supercritical flow region, the main flow lifts to the water surface. In the transition from supercritical to subcritical flows, a submerged flow with a surface roller does not occur, and a surface jet flow is formed. The main flow rises to the water surface easily.

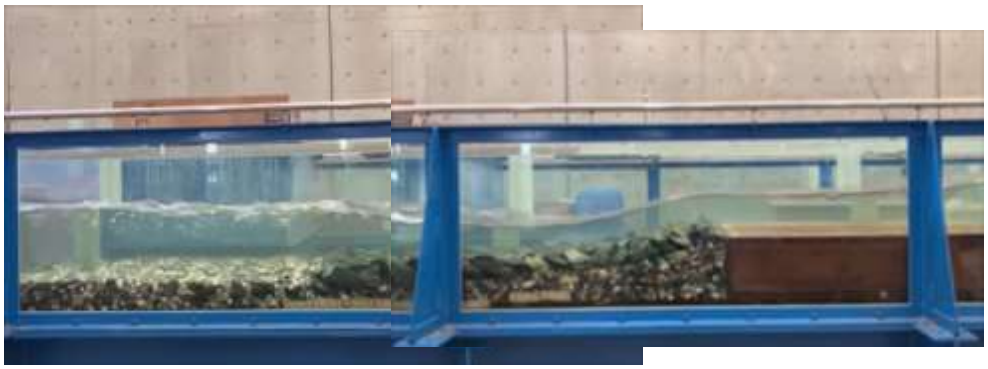

Figure 26. Flow condition at ramp with assembled boulders

Regarding the water surface profiles during a flood stage, as shown in Figure 27, an undular surface forms in the transition from supercritical to subcritical flows. Then, X is horizontal streamwise coordinate from upstream end-section of assembled boulders, y is transverse coordinate from the center of channel, and Z is elevation from the channel bottom. The circle and triangular marks show the position of the maximum velocity Zmax. The position of maximum velocity is always located near the water surface in the transition from supercritical to subcritical flows. The downstream water level adjusted to transit from supercritical to subcritical flow at the end section of assembled boulders. In addition, the downstream depth is almost same as in the case of jump formation just below vertical drop.

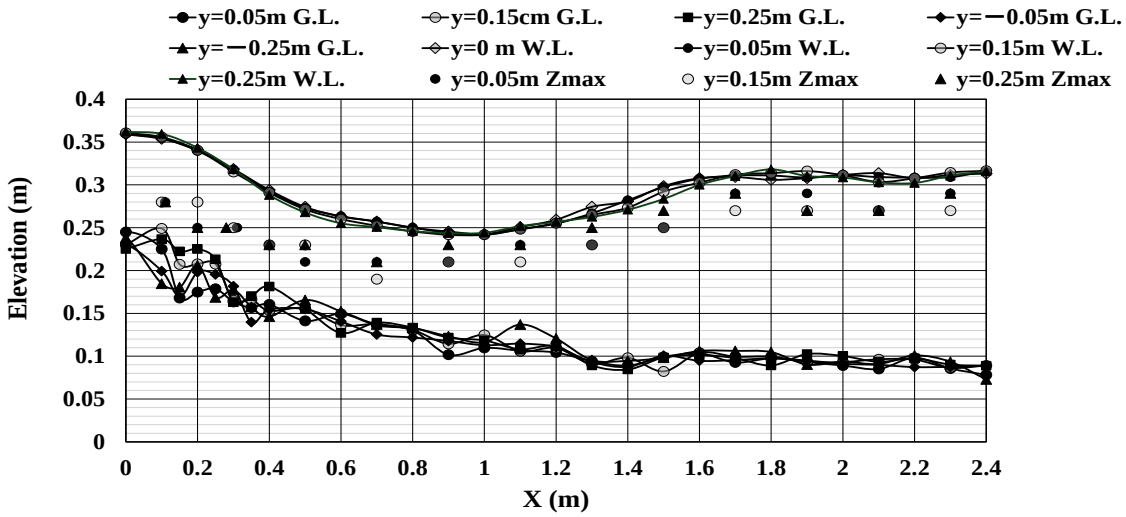

Figure 27. Streamwise change of position of maximum velocity defined at each section

Figure 28 shows streamwise change of maximum velocity at each vertical section. Then, um is maximum velocity with X-component. As shown in this figure, the maximum velocity increases up to the section where X = 0.8-1.0 m, and the maximum velocity decays gradually in the transition from supercritical to subcritical flows. The velocities near the side can reduce at the downstream of the assembled boulders because the installation shape of the assembled boulders is parabolic (see Figure 24).

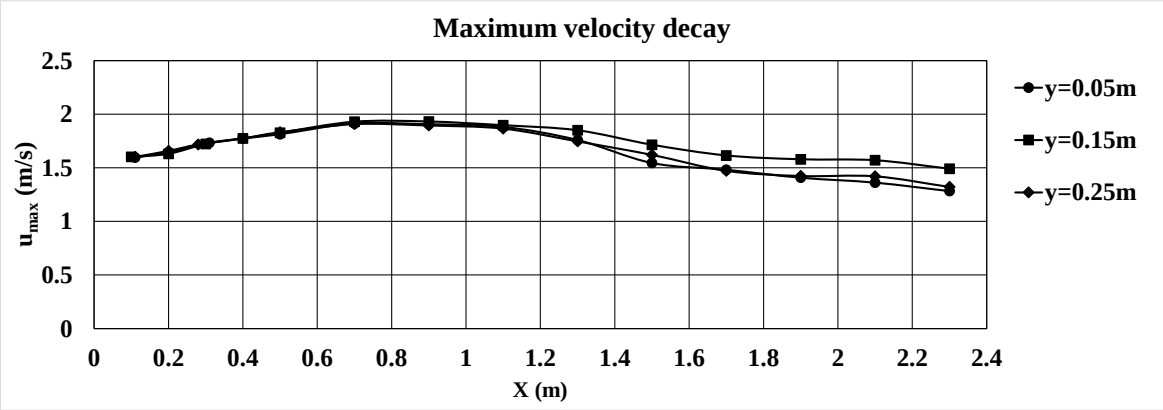

Figure 28. Streamwise change of maximum velocity evaluated at each vertical section

Figure 29 shows the change in the direction of the streamlines of the X component velocity near the bottom. Since the direction of the flow that has just passed over the ramp approaches parallel to the slope, the X component velocity decreases in the range of $0 < X(m) < 0.4$. Subsequently, the mainstream in supercritical flow region rises, causing the flow to accelerate. In the range of $0.5 < X(m) < 1.3$, the velocity near the bottom decreases due to the low velocity of the seepage flow. In the range of $1.4 < X(m) < 1.8$, as the flow transits from supercritical to subcritical flows, local flow effects cause deceleration and acceleration of the bottom velocity. In all cases, the flow velocity near the bottom is approximately 0.2 m/s, which is not sufficient to cause scouring.

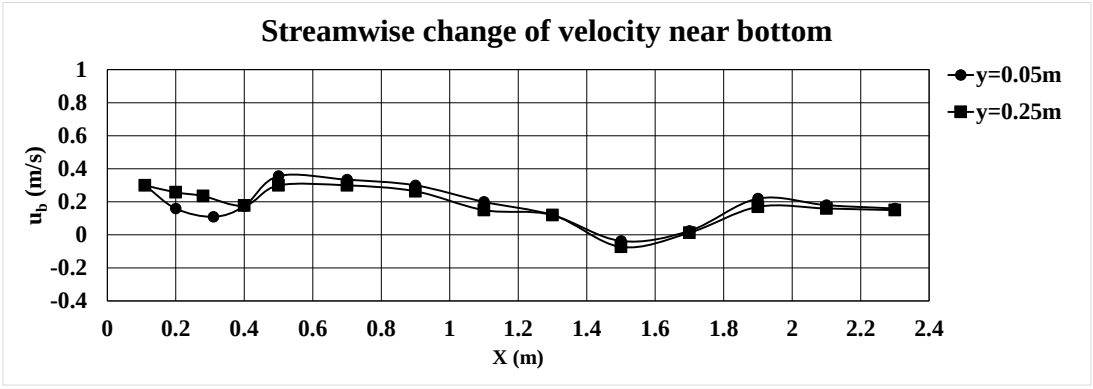

Figure 29. Streamwise change of velocity near bottom

Figure 30 shows velocity profiles in supercritical flow region ($0.1 < X(m) \leq 0.4$). Separated flow with air entrainment forms by inserting the probe with 4 mm diameter into a high velocity flow. It is impossible to measure the velocity by using electrical magnetic velocity meter, supporting the velocity measurement for X component above assembled boulders by propeller velocity meter. u and v are time averaged velocities for X and y components, respectively. u' and v' are standard deviations (representing turbulent intensities) for X and y components, respectively. In these profiles, the seepage flow region includes. In seepage flow inside boulders and crushed stones, all velocities including turbulent intensities are always small.

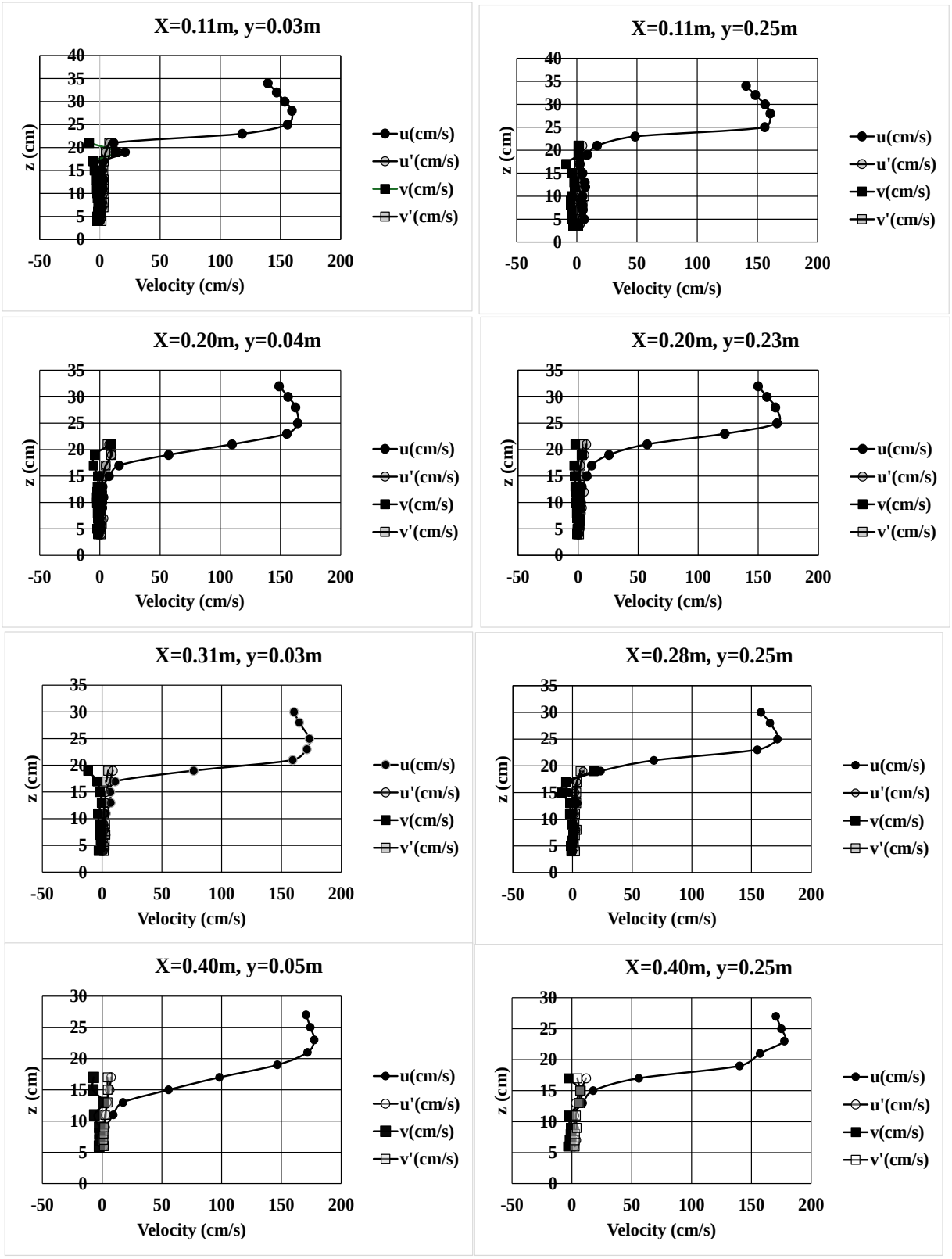

Figure 30. Velocity profiles at installation region of assembled boulders

Figure 31 shows velocity profiles above consecutively assembled boulders in supercritical flow region to find velocity decay near the bottom. This figure includes Equations (1) and (2) for comparison with the flow in a normal open channel.

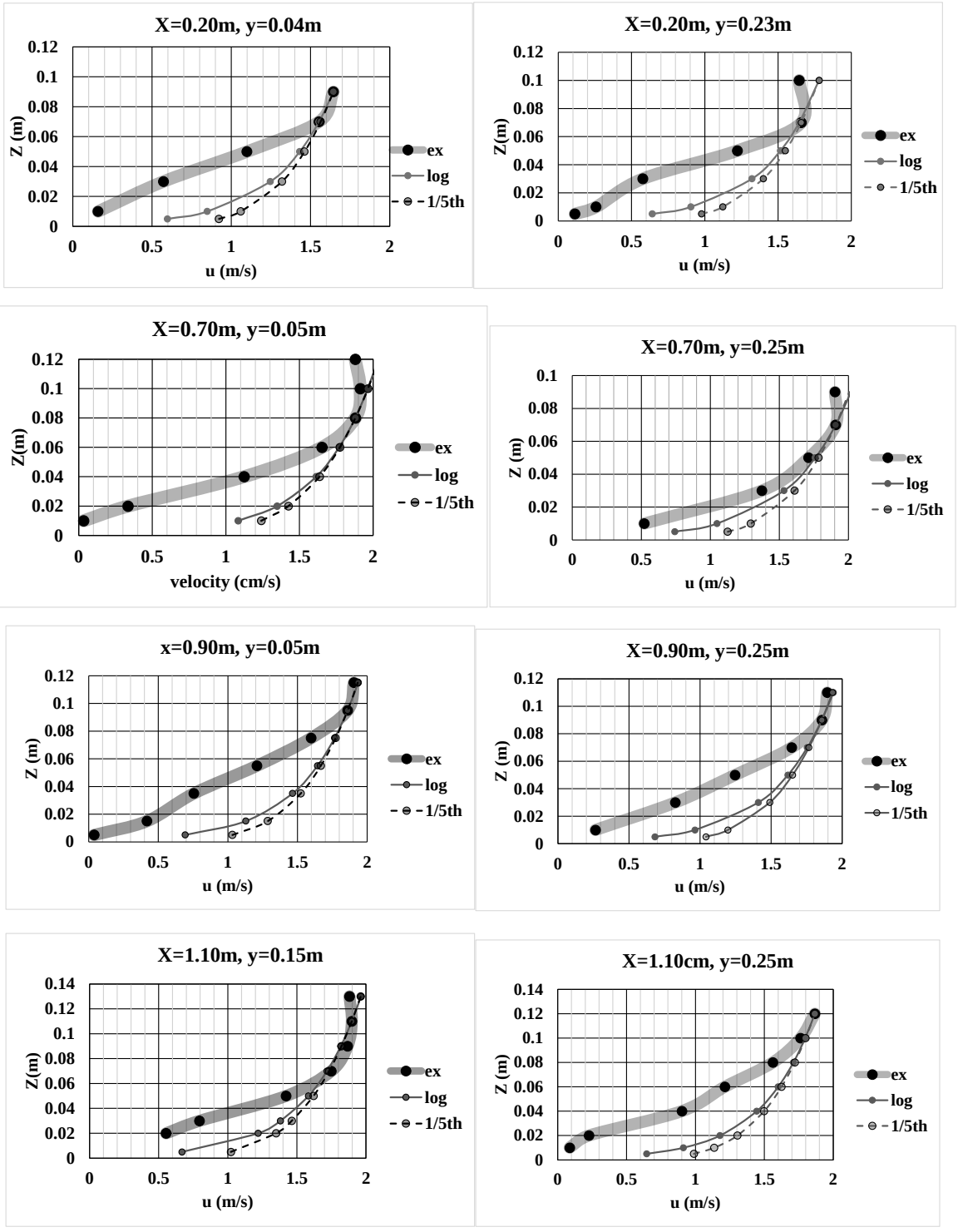

Figure 31. Velocity profiles above consecutively assembled boulders in supercritical flow region

$$\frac{\bar{u}}{V_*} = 5.75\, Log\left(\frac{Z}{k_S}\right) + 8.5 \quad (1)$$

$$\frac{\bar{u}}{u_m} = \left(\frac{Z}{Z_m}\right)^{1/5} \quad (2)$$

Then, Equation (1) is logarithmic law equation applied for turbulent flow on roughness (CHOW, V.T. 1959). Equation (2) is 1/5th power law equation approximated to stepped channel flow (Ohtsu and Takahashi 2012) and may be applied to a open channel flow in large roughness bed. In these equations, k_s is average roughness height from reference point, $\bar{u}$ is time average velocity for streamwise component, u_m is maximum velocity, V_* is friction velocity, X is horizontal coordinate from the upstream end of ramp with assembled boulders, y is transverse coordinate from center of channel, Z is vertical coordinate from reference point, and Z_m is the height from reference point to maximum velocity.

The reference point (Z = 0) is defined as an upper limit of seepage flow region at each measurement section (see Figure 30). The friction velocity predicts by substituting the maximum velocity um and its position Z to equation (1).

As shown in Figure 31, the velocity profile is different from that predicting from equations (1) and (2), the value of the velocity near the bottom is always smaller by the shape of assembled boulders and the formation of seepage flow inside the boulders.

Figure 32 shows velocity profiles including seepage flow region (X = 0.20 m and y = 0.23 m). The standard deviations (e.g., turbulent intensity) for both components reduce in seepage flow region. Also, the standard deviation is still smaller even if the measurement points above boulders approach near the surface of boulders. As the boulders arrange in a staggered pattern, the velocity of the seepage flow inside boulders becomes smaller. As a result, time-average velocity and its standard deviation can be reduced inside the assembled boulders.

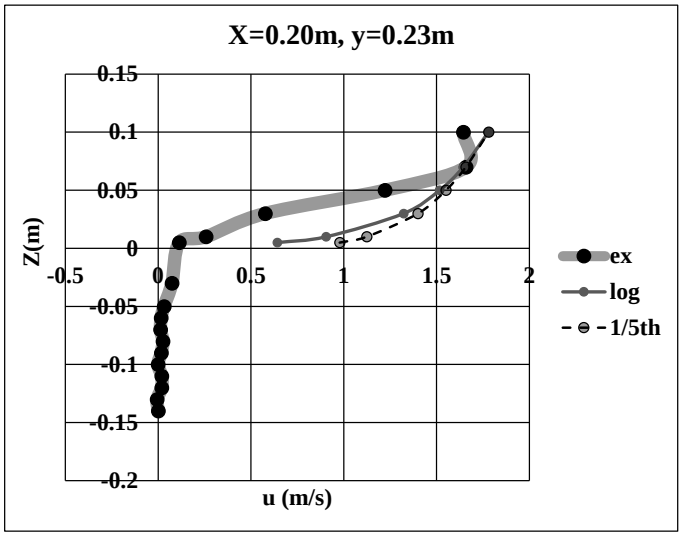

Figure 32. Velocity profile including seepage flow region (X = 0.20 m and y = 0.23 m)

In accordance with the experimental evidence, the prototype of the ramp with the assembled boulders was constructed. As shown in Figures 33 to 35, several sizes of boulders were used in the constructions, because the size of transported boulders and driftwood during flood stages depends on the installation location.

Figure 33. Flow condition at ramp with consecutively assembled boulders in prototype (1/4 slope)

Figure 34. Construction of ramps with assembled boulders and protection region

Figure 35. Flow condition at ramp with consecutively assembled boulders in prototype (1/10 slope)

In low drop structure with 3.5 m height, it is impossible for swimming and benthic fishes and crustaceans to migrate upstream, but the ramp with the assembled boulders was assisted for both upstream and downstream migrations of multi-aquatic animals. In the ramp shown in Figures 33 and 34 located in Kanna river, Gumma prefecture, most swimming and benthic fishes could migrate upstream by utilizing the flow between boulders. This result was confirmed by surveys of populations of fishes immediately downstream of the drop structure. Before improvement, fish passages were installed on both sides, but thousands of swimming fishes and benthic fishes were stagnating in the stilling basin immediately below the drop structure.

At the check dam shown in Figure 35 located in Shiretoko peninsula, Hokkaido, the installation of a ramp with assembled boulders enabled various fish species inhabiting the watershed and fish migrating from the estuary to move upstream. This was confirmed by field observations at the stilling basin immediately downstream of the unimproved next check dam.

There was no necessity of maintenance in the ramp with the assembled boulders since the construction. The ramp was no obstacle for both upstream and downstream migrations of multi-aquatic animals. Further, there was no severe local scouring downstream of the ramp. In addition, the riverbed downstream of the constructed ramp consists of a variety of boulder sizes, which may have had a similar effect of the installation of crushed stones.

6. Slit-Type Check Dam

The physical model shown in Figure 36 installed on a channel 15 m long and 0.80 m wide to investigate the improvement of flow conditions downstream of a check dam by installing consecutively assembled boulders below the sub-dam. Furthermore, crushed stones were installed downstream of the assembled boulders as a protection zone. The scale of the model was set to 1/10, applying the Froude similarity. Based on the model scale, the discharge equivalent to the design discharge was set to Q = 0075 m^3/s. Figure 37 shows the flow condition downstream of the check dam and around the assembled boulders under a design discharge. As shown in Figure 37 (a), in the slit-type check dam, a hydraulic jump with a large amount of air entrainment in a stilling basin. In the stilling basin, the main flow does not reduce sufficiently, and a high-velocity flow impinges on the upstream face of sub-dam, forming an upwelling flow on both sides. As a result, the upwelling flow became significant, and a three-dimensional surface jet flow formed downstream of the sub-dam. By installing the assembled boulders as parabolic shape, as shown in Figure 37 (b), the main flow rapidly rises toward the water surface, and a surface jet flow with undulation occurs. During the 70-hour flow period from the start to the end of the experiment, there were no movement of crushed stones. As shown in Figure 37 (c), focusing on the flow around the installation of assembled boulders, the boulders arranged in a staggered pattern, controlling the flow velocity near the top of the bottom and preventing air bubbles from penetrating inside stones.

Figure 36. Physical model of assembled boulders and crushed stones

(a) Flow condition around a stilling basin

(b) Flow condition at downstream of sub-dam

(c) Aerated flow above the assembled boulders

Figure 37. Flow condition at downstream of slit-type check dam

Figure 38 shows a definition sketch of physical model. The installation area for the assembled boulders was set as 0.8 m with slope (1/10 gradient) and a 0.5 m horizontal section, and crushed stones were set to 1.8 m long. The length of stilling basin and the height of sub-dam were determined under a design discharge (Q = 0.075 m3/s in scale model). The width of the slit was set so that the upstream water level reached the top of the check dam. The transverse bottom profiles in horizontal zone of the assembled boulders were set as parabolic shape. Figure 39 shows the maximum time-average velocity decays downstream of the sub-dam. In the upstream part of the slope, acceleration occurs because the flow has just overflowed from the sub-dam, but the maximum flow velocity decreases as the supercritical flow passes through the assembled boulders zone. Further, the flow deflects from side to center, and the maximum velocity decays near the side is larger than that near the center part. As shown in Figure 40, the flow passing over the slope is supercritical flow, and the undulation surface continues far downstream by the formation of a surface jet flow. The difference of the water surface profiles at y = 0 m and 0.25 m is small. The location of the maximum time average velocity um evaluated at each vertical measurement section is away from the bottom (Figure 40). As a three-dimensional flow continues far downstream, the location of um at y = 0.37 m (near side) is lower than that at y = 0 m (center).

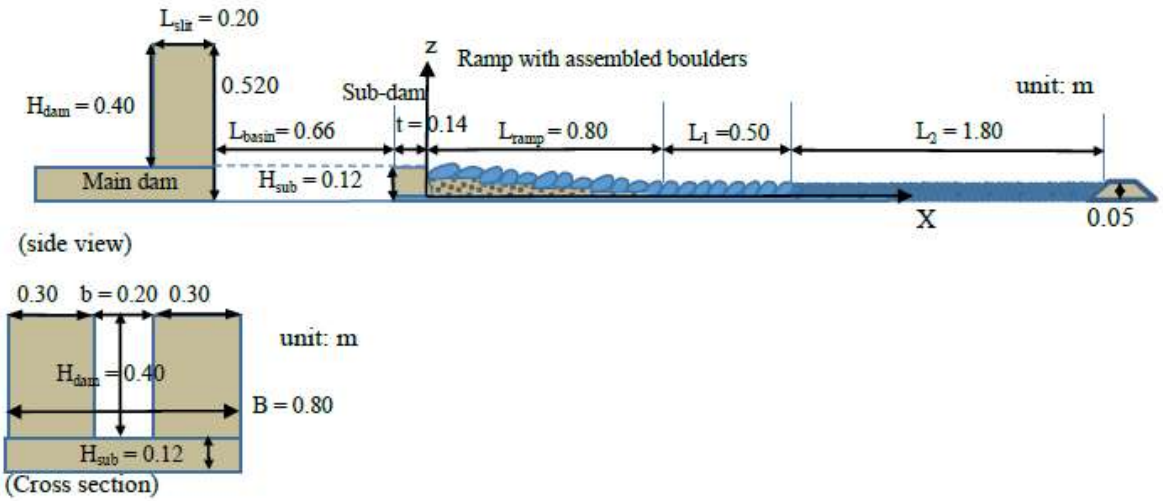

Figure 38. Physical model of slit type check dam

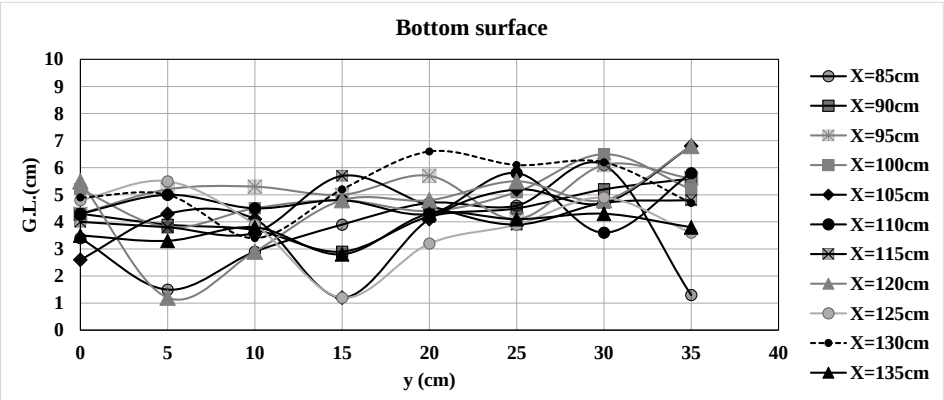

Figure 39. Transverse bottom profiles in protection region due to assembled boulders

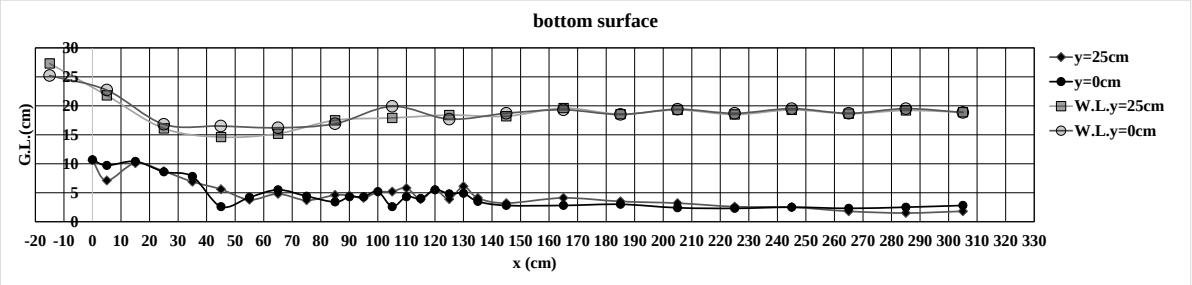

Figure 40. Water surface and bottom profiles downstream of sub-dam for streamwise direction

Figure 41 shows the streamwise change of the time-average flow velocity near the bottom at the downstream of the sub-dam. In the installation area of the assembled boulders, the time-average flow velocity varies due to the unevenness of the boulders and the seepage flow inside the boulders. At the downstream part of the assembled boulders, the rise of the main flow decreases, causing a slight acceleration in the flow velocity near the bottom. However, the flow velocity is suppressed to about 20 cm/s due to the influence of seepage inside the crushed stones. Regarding the standard deviation (i.e., turbulent intensity) near the bottom, as shown in Figure 43, the difference depending on the transverse position is small, and the turbulence intensity (standard deviation) decreases to approximately 10 cm/s at the downstream part of the crushed stones.

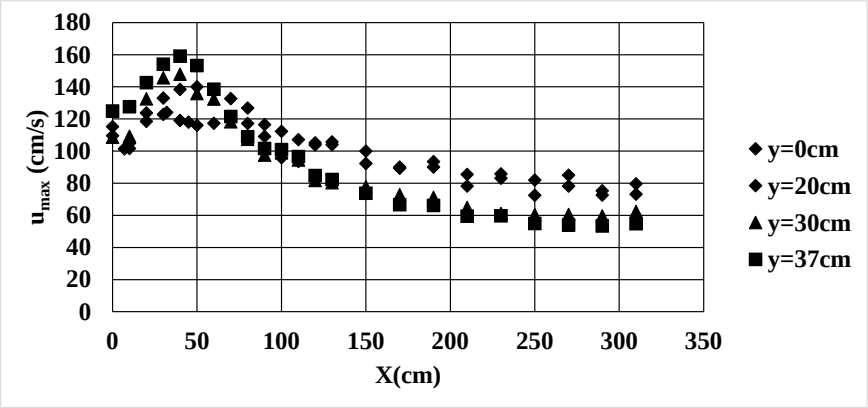

Figure 41. Maximum velocity decay downstream of sub-dam

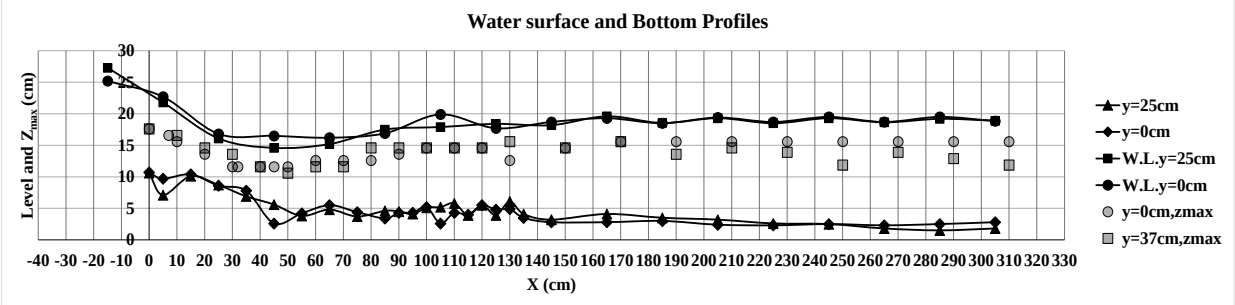

Figure 42. Development of main-flow position downstream of sub-dam

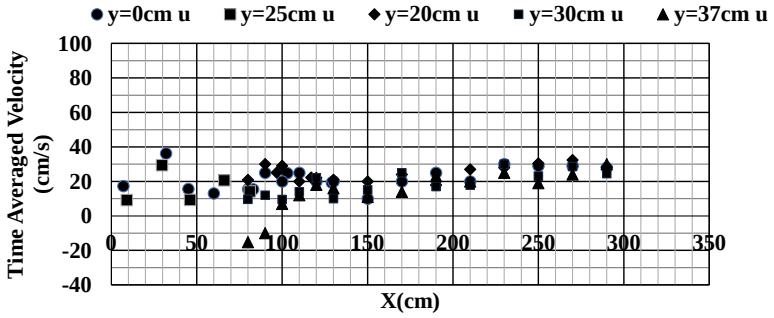

Figure 43. Streamwise change of time averaged velocity near the bottom

Figure 44 shows the velocity profiles downstream of the ramp region. In the assembled boulders area, the vertical distribution of flow velocity and the velocity gradient du/dz are different from those in the crushed stones area and are smaller. The unevenness of the large boulders may promote the upward flow of the mainstream. Also, in the crushed stones area, seepage effects may help the reduction of the time average flow velocities and the standard deviations for downward direction. Figure 45 shows the velocity profiles including seepage flow region. The time average flow velocities and standard deviations within the seepage flow area are always small, contributing to the control of flow velocity near the bottom surface.

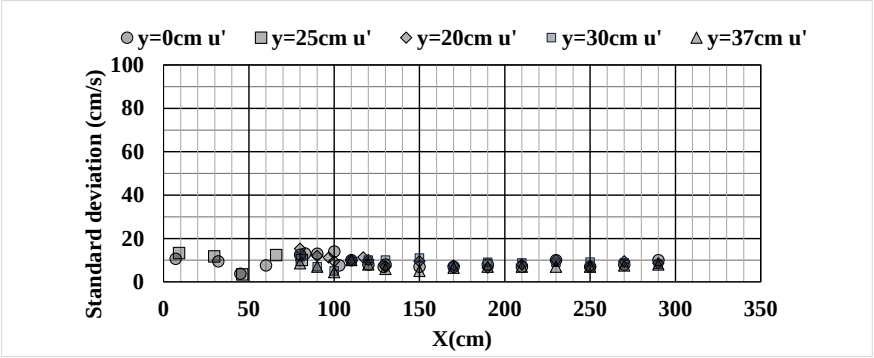

Figure 44. Streamwise change of standard deviation for velocity near the bottom

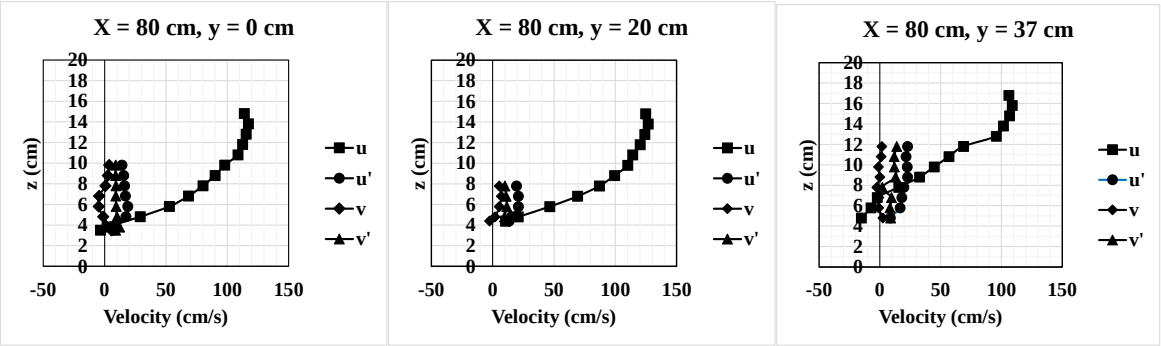

(a) $X/L_{ramp} = 1.00$

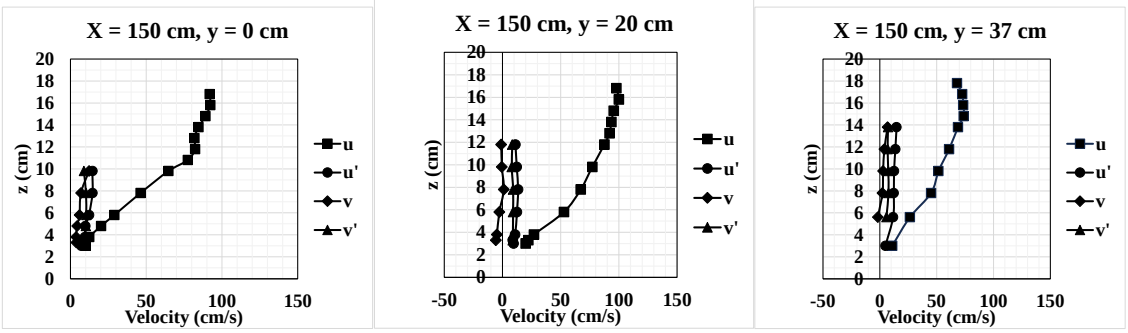

(b) $X/L_{ramp} = (L_{ramp} + L_1)/Ls + (X-L_{ramp}-L_1)/L_{ramp} = 1.625 + 0.250 = 1.875$

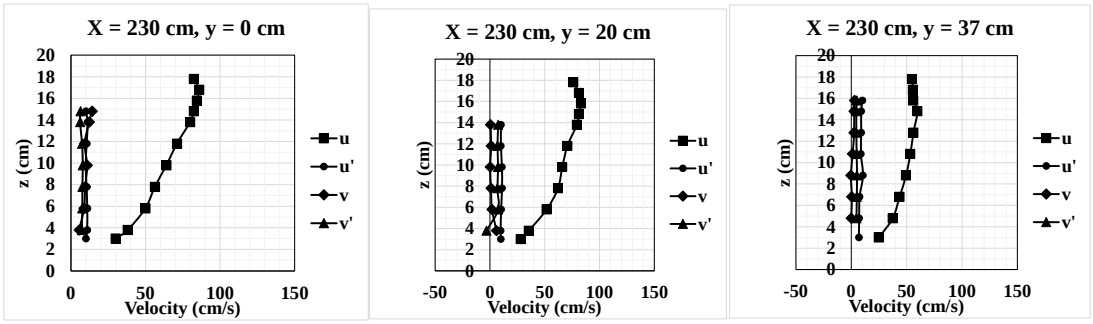

(c) $X/L_{ramp} = (L_{ramp}+L_1)/L_{ramp} + (X-L_{ramp}-L_1)/L_{ramp} = 1.625 + 1.250 = 2.875$

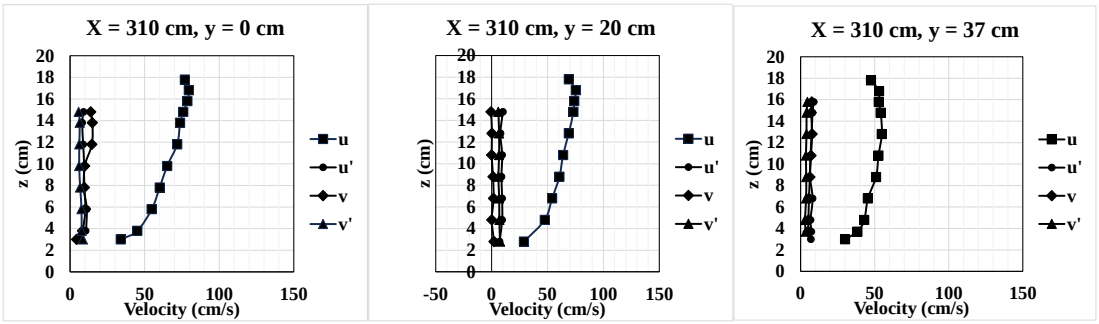

(d) $X/L_{ramp} = (L_{ramp}+L_1)/L_{ramp} + (X-L_{ramp}-L_1)/L_{ramp} = 1.625 + 2.250 = 3.875$

Figure 45. Velocity profiles at each section at y = 0, 20, and 37 cm

Therefore, appropriate placement of assembled boulders and crushed stones enables the rise of the main flow, moderates flow velocity near the bottom surface, and leads to the prevention of local scouring.

7. Bridge Pier

Yasuda and Ishitsuka (2024) proposed the installation of the consecutively assembled boulders to protect local scouring around bridge pier. In this experiment, the measurements of the water surface profile, riverbed profile and flow velocity were taken at a model discharge of Q = 0.150 m^3/s, assuming a flood stage. The average size of the boulders was set 0.092 m in the installation of assembled boulders. In the protection region downstream of the assembled boulders, crushed stones with 0.016 m average size were used. The average size of 0.0053 m pebbles was used to investigate the possibility of local scouring downstream of protection region. The downstream depth was set as a depth slightly greatear than that at which pebbles naturally begin to move at the set discharge (0.150 m^3/s) when only pebbles are installed in the channel. The experimental investigation revealed that the seepage flow inside assembled boulders may help the reduction of the flow velocity near the bottom. The collision with the cylinder caused a deflected flow to form, resulting in a higher flow velocity on the side wall than in the center of the channel, with the effect extending far downstream. After more than 20 hours have elapsed since the start of the experiment, local scouring occurs downstream of the installation region due to the assembled boulders. Then, the authors propose the installation due to crushed stones downstream of the assembled boulders as shown in Figure 46, and the flow velocity near the bottom will decrease due to the seepage flow inside the crushed stones. Further, the transverse installation shape of the assembled boulders is

parabolic to reduce the deflected flow near the side (Figure 47). At the upstream of the bridge pier, the installation length due to pebbles is set to 0.50 m long and the thickness is 0.05 m (Figure 48). The upstream end part of the pebbles was a reverse slope with crushed stones to reduce the water surface gradient. The physical models were set to 1/6 scale under the Froude similarity. Figure 49 shows the flow condition passing over the pier. For both cases of two-cylindrical piers (Figure 49 (a)) and a long elliptical pier (Figure 49 (b)), water surface has stable undulation caused by a deflected flow due to the collision with the pier. Downstream of these stable waves, the water surface becomes unstable, and there is no time-average undulation. If the installation region due to crushed stones will cover with the unstable region, there is no local scouring for a long time. Figure 50 shows definition sketch for both cases of two-cylindrical piers and a long elliptical pier. The lengths L_1, L_2, L_3 were set to 0.54 m, 1.4 m, and 0.8 m, respectively. In addition, the installation length of the assembled boulders was set to 1.0 m. The installation length due to crushed stones is longer than that due to the assembled boulders downstream of pier. As the porosity ratio of crushed stones with average size 0.0163 m is smaller than that of boulders with average size 0.090 m, the seepage flow inside crushed stones may reduce the flow velocity near the bottom.

Figure 46. Installation of assembled boulders, crashed stones, and pebbles stones

Figure 47. Parabolic shape of assembled boulders

Figure 48. Installation of consecutively assembled boulders around long ellipse pier

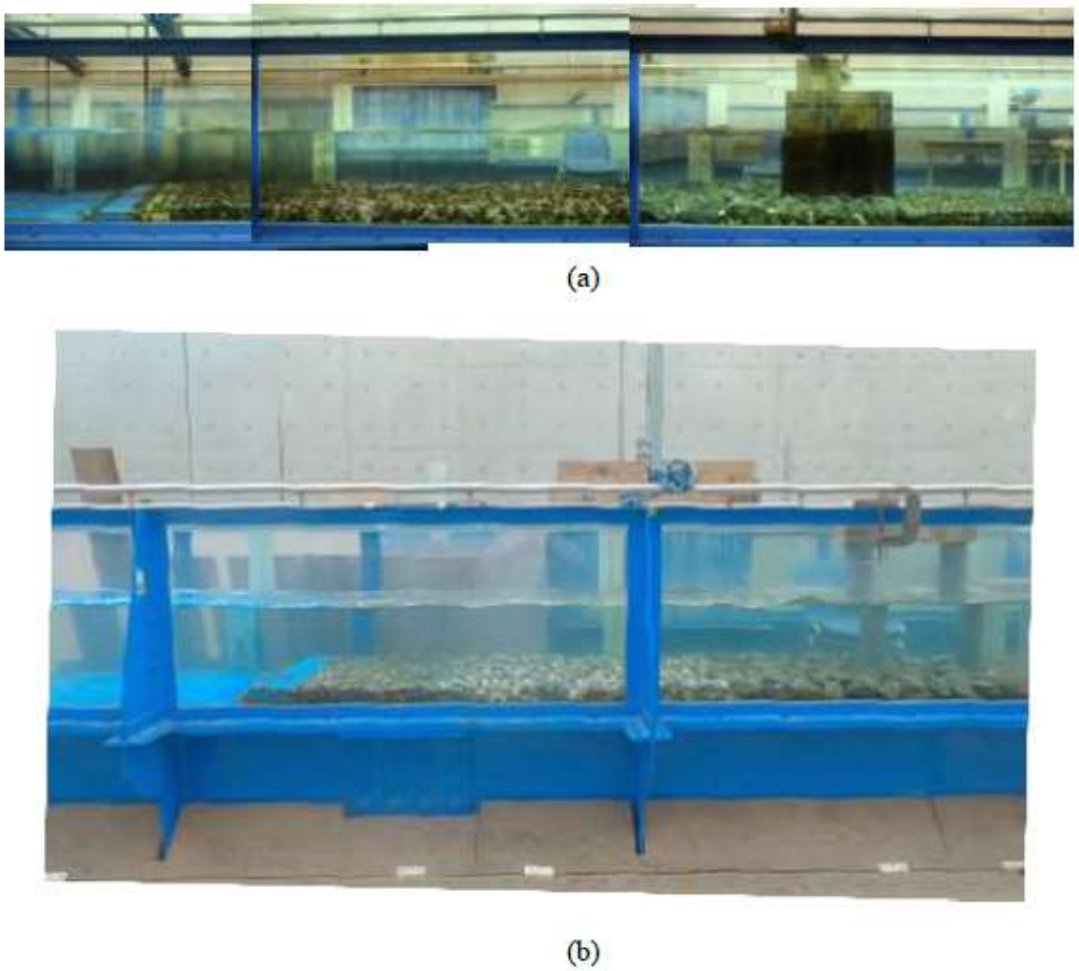

(a) Long elliptical pier, (b) Two cylindrical piers

Figure 49. Flow conditions passing over piers

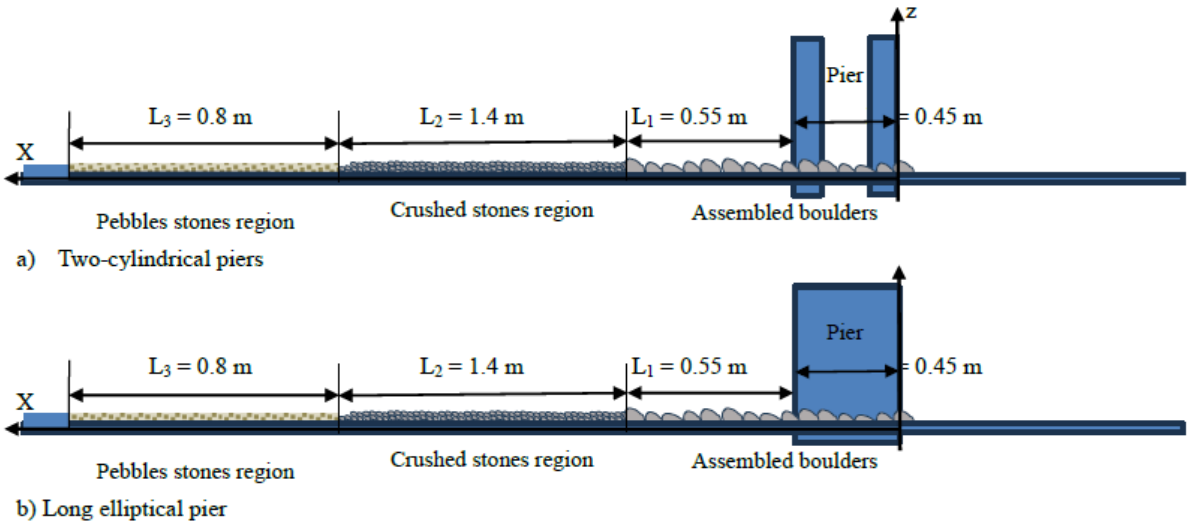

Figure 50. Bridge cylindrical piers model

Figures 51 and 52 show streamwise change of velocity profiles for the time-average flow velocity u at each vertical section. As shown in these figures, the velocity profiles are different between y = 0 m and y = 0.32 m, the time-average flow velocity of the main flow at y = 0.32 m is always larger than that at y = 0 m at the downstream of the pier. The main flow at the center (y = 0 m) rises toward water surface downstream of the assembled boulders. On the other hand, the position of the main flow near the side (y = 0.32 m) changes to downward downstream of the assembled boulders. There are no different velocity profiles between two-cylindrical piers and a long elliptical pier. Accordingly, the deflected flow formed by the collision with the pier should not be negligible even if the flow is passing through the installation region due to crashed stones. The reduction of the flow velocity by seepage flow inside crushed stones must be significant as the protection method against local scouring.

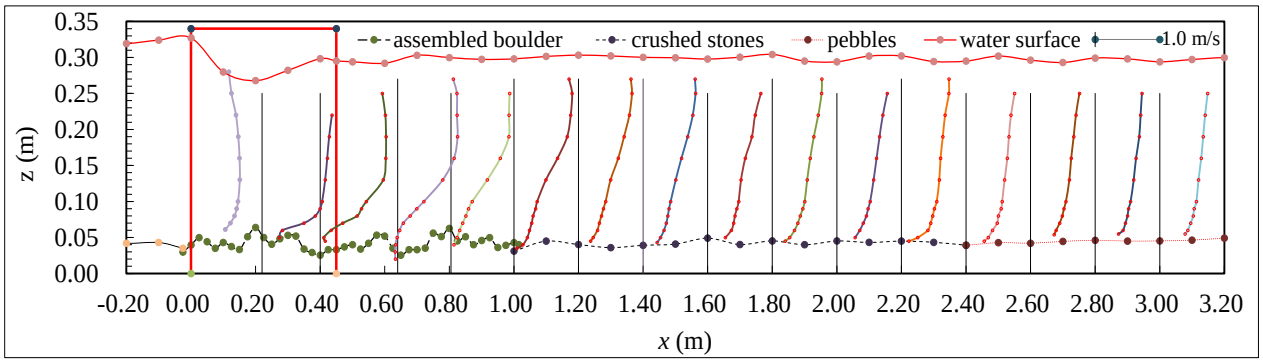

(a) y = 0.09 m

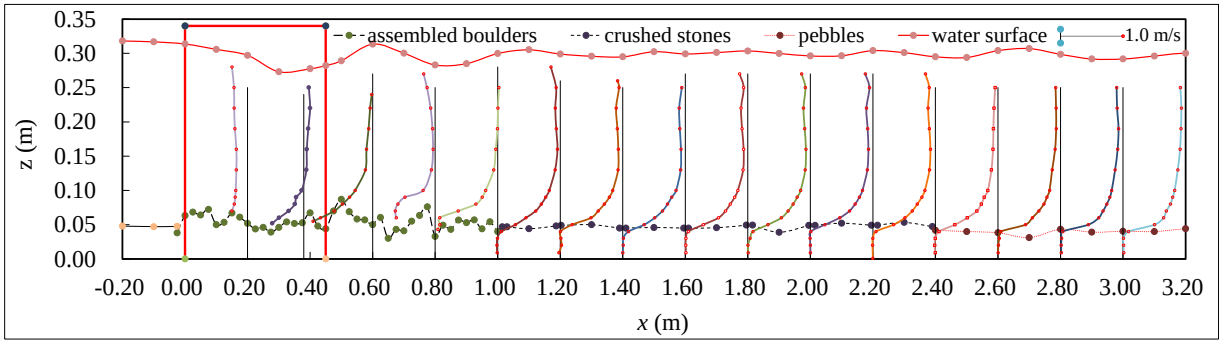

(b) y = 0.32 m

Figure 51. Velocity, water surface, and bed profiles in case of long elliptical pier

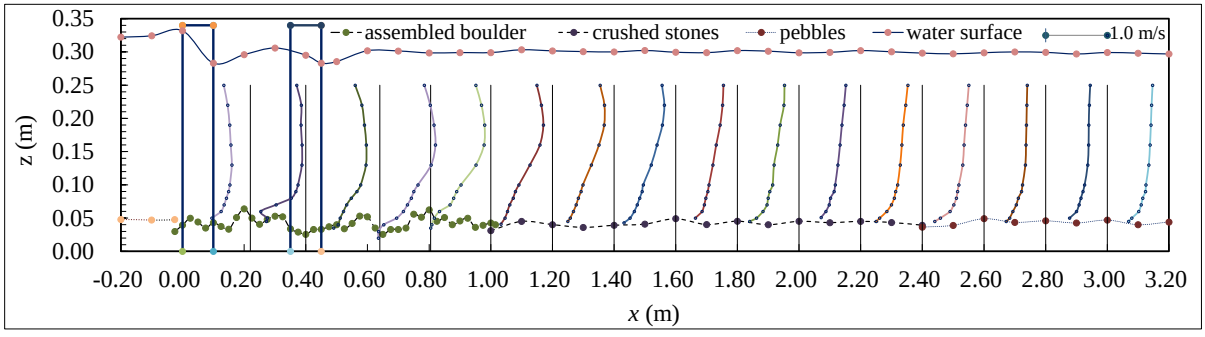

(a) y = 0.09 m

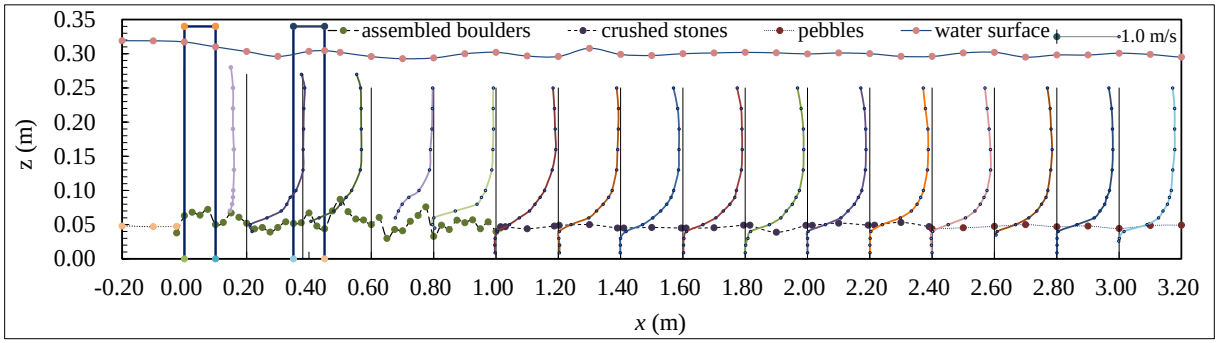

(b) y = 0.32 m

Figure 52. Velocity, water surface, and bed profiles in case of two cylindrical piers

Figures 53, 54, and 55 show velocity profiles at X = 1.0 m (downstream end of installation due to assembled boulders), 2.2 m (0.2 m downstream from upstream end of installation due to crushed stones), and 3.0 m (0.2 m downstream from downstream end of installation due to crushed stones). As shown in these figures, the standard deviations u' and v' decrease near the bottom and the values of u' and v' inside stones are almost zero. The time-average flow velocity at y = 0.32 m is always larger than that at y = 0 m under given measurement level z. The velocity gradient du/dz at y = 0.32 m near the bottom is larger than that at y = 0 m and it might be easier to increase the time-average flow velocity, resulting in the occurrence of local scoring. The formation of the seepage flow inside either crushed stones or pebbles is the most significant for the reduction of the flow velocity including turbulent intensity (i.e., standard deviation) even if the effect of the deflected flow on the time-average flow velocity near the bottom is large.

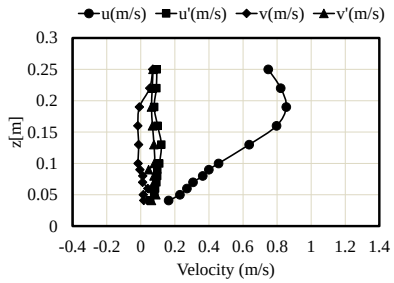

(a) y = 0.09 m two cylindrical piers

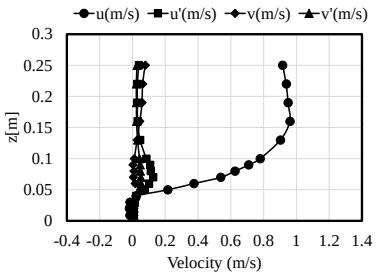

(b) y = 0.32 m two cylindrical piers

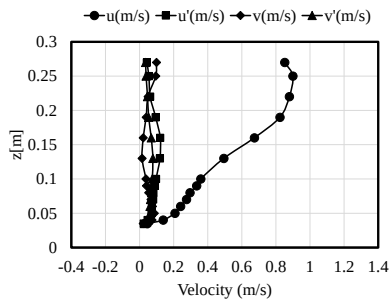

(c) y = 0.09 m long elliptical pier

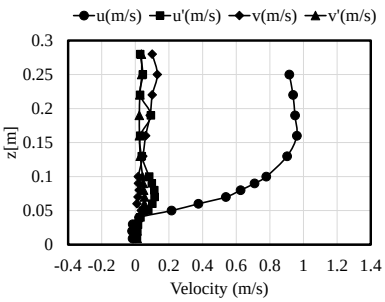

(d) y = 0.32 m long elliptical pier

Figure 53. Velocity profiles at X = 1.00 m downstream of pier

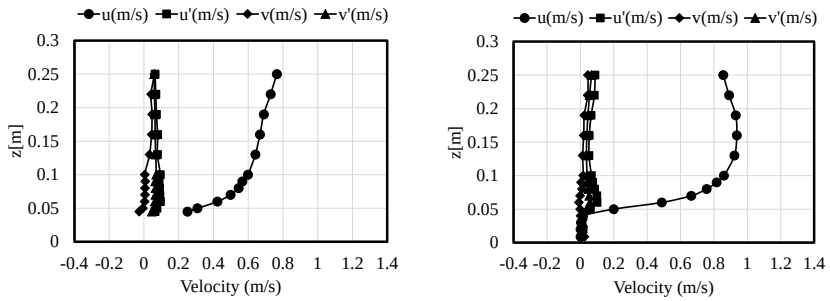

(a) y = 0.09 m two cylindrical piers (b) y = 0.32 m two cylindrical piers

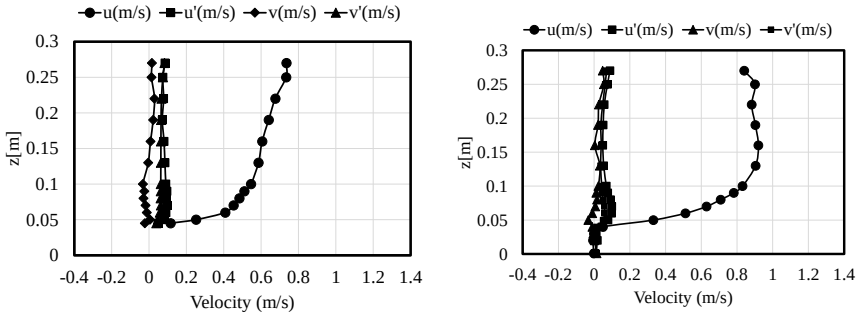

(c) y = 0.09 m long elliptical pier (d) y = 0.32 m long elliptical pier

Figure 54. Velocity profiles at X = 2.22 m downstream of two cylindrical piers

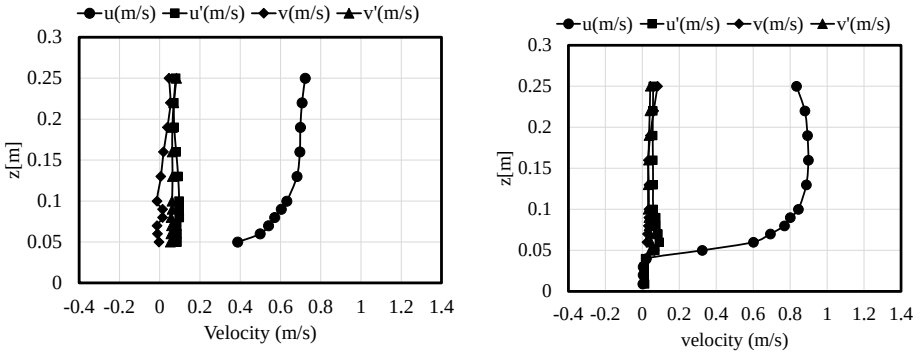

(a) y = 0.09 m two cylindrical piers (b) y = 0.32 m two cylindrical piers

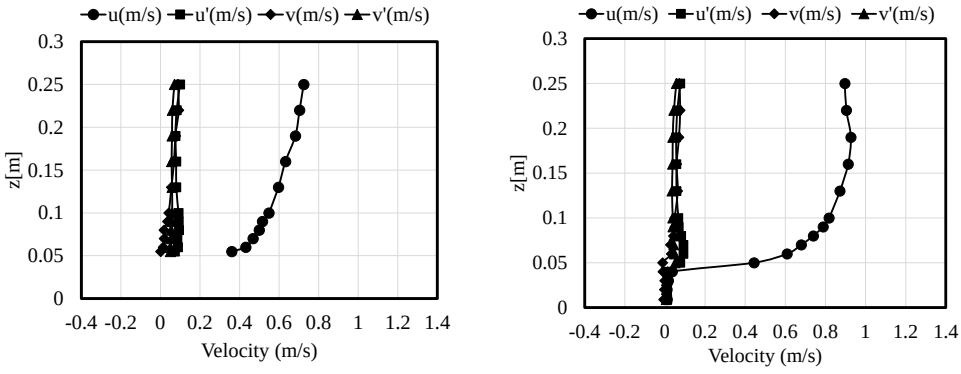

(c) y = 0.09 m long elliptical pier (d) y = 0.32 m long elliptical pier

Figure 55. Velocity profiles at X = 3.00 m downstream of long elliptical pier

Figure 56 shows the application of the installation due to the assembled boulders in Okkabake river, Hokkaido, Japan. In November 2024 to January 2025, as a first construction, the construction engineers consecutively assembled boulders around a long elliptical pier for both the prevention of the pier and the improvement for the migration of aquatic animals in accordance with the author's design. The bridge is located near the river mouth and the riverbed formed by pebbles and crushed stones, and boulders. Unusual snowfall covered the watershed area of Okkabake river during the winter season, and a big flood occurred in April. After the flood, there was no local scouring, and the flow condition around the installation region does not interfere against the upstream and downstream migration of multi-aquatic animals and is safe for people to approach.

(a) (b)

Figure 56. Long elliptical pier with assembled boulders protection in Okkabake river, Hokkaido

8. Conclusions

The installation of consecutively assembled boulders is applicable for the improvement of flow conditions around several types of hydraulic structures, not only for the improvement of river flow conditions. During a normal stage, the flow condition passing over the assembled boulders forms several types of flows and seepage flows inside boulders, and for multi-aquatic animals, the flow condition around assembled boulders may be helpful as the upstream downstream migrations, habitat, and refuge. During flood stages, the combination of the assembled boulders and the crushed stones is helpful for the energy dissipation and effective for the bed protection against local scouring. The effect of the installation of the assembled boulders on the velocity reduction near the bottom shows from the experimental results on movable weir with support pillar, abrupt drop structure, ramp with the assembled boulders, slit-type check dam, and bridge piers. Then, the formation of seepage flow inside boulders is the most significant for the reduction of the velocity near the bottom. Further, the unevenness of the large boulders may promote the upward flow of the mainstream. Flows around hydraulic structures form deflected flows in addition to the three-dimensional flow characteristics. Particularly in areas where deflected flow significantly impacts the flow condition in subcritical flow, countermeasures against scouring, utilizing not only the installation of the assembled boulders but also the formation of seepage flows inside crushed stones, becomes crucial.

In the case of movable weir with support pillar, the deflected flow formed by impinging against the pillars significantly impacts the flow condition in subcritical flow during flood stages, and the installation of the assembled boulders and crushed stones as protection area helps the protection against local scouring.

For an abrupt drop structure, during flood stages, the deflected flow formed by impinging on the apron makes a three-dimensional structure flow. The main flow continues near the bottom far downstream even if hydraulic jump is formed. The installation of the assembled boulders supports the reduction of the flow velocity near the bottom due to the formation of seepage flow, and the parabolic shape in the installation area assists the lift of the main flow toward to the water surface.

In the case of ramps with the assembled boulders, the structure of the installation is the most significant for both the stabilization of the boulders and the velocity reduction near the bottom during flood stages and for the upstream migration of multi-aquatic animals during normal stages. The formation of seepage flow inside the assembled boulders is effective for both flood and normal stages.

The formation of the surface jet flow is effective against the local scouring downstream of sub-dam in a slit-type check dam during flood stages. The installation of the ramps with the consecutively assembled boulders below

sub-dam enables the formation of the surface jet flow. On the other hand, a deflected flow formed by impinging on the upstream face of the sub-dam affects the velocity near the bottom downstream of the assembled boulders. The installation of crushed stones downstream of the assembled boulders helps the velocity reduction due to seepage flow near the bottom. Further, the parabolic shape in the installation area of the assembled boulders assists the rising of the main flow toward to water surface and the velocity reduction near the side. The combination of the assembled boulders and crushed stones is the most important for the prevention of riverbeds during flood stages. The prototype of the ramps proves experimental results.

A deflected flow due to impingement to the front of bridge piers makes local scouring during flood stages and forms a three-dimensional flow in which the main flow locates near the bottom far downstream. The installation of the assembled boulders around pier helps the prevention of local scoring around piers. Further, the installation of crushed stones downstream of the assembled boulders should be recommended, because the seepage flow inside crushed stones makes the flow velocity reduction near the bed. The combination of the assembled boulders and crushed stones is the most significant for the protection against local scouring and preservation of refuge and habitat for multi-aquatic habitat during normal stage.

References

Breusers, H. N. C., & Raudkivi, A. J. (1991). *Scouring. Hydraulic Structures Design Manual Series*, Vol. 2, IAHR. Rotterdam: A. A. Balkema.

Chaudhary, R. K., Sharma, N., & Ahmad, Z. (2021). Block ramps for stream power attenuation in gravel-bed streams, *Water Supply, 21*(2), 493-510. https://doi.org/10.2166/ws.2020.339

Chiew, Y. M. (2002). Failure mechanisms of riprap layer around bridge piers. *Proceedings First International Conference on Scour of Foundations, ICSF-1, Texas A&M University, College Station, Texas, USA November 17-20*, pp.70-91.

Chow, V. T. (1959). *Open channel hydraulics.* McGraw-Hill, New York.

Engineering Manuals & Monographs. (2022), *Hydraulic Laboratory Publications (Entire Collection), Technical Service Center.* Technical Reports, TSC Home, USBR, Mar 14. Retrieved from https://www.usbr.gov/tsc/techreferences/hydraulics_lab/pubs/manuals_monographs.html

Ettema, R., Kirkil, G., & Muste, M. (2006). Similitude of largescale turbulence in experiments on local scour at cylinders. *Journal of Hydraulic Engineering, 132*(1), 33-40. https://doi.org/10.1061/(ASCE)0733-9429(2006)132:1(33)

Farhoudi, J., & Smith, K. V. H. (1985). Local scour profiles downstream of hydraulic jump, *Journal of Hydraulic Research, 23*(4), 343-358. https://doi.org/10.1080/00221688509499344

Hager, W. H. (1992), *Energy dissipators and hydraulic jump, Water Science and Technology Library.* Kluwer Academic Publishers. https://doi.org/10.1007/978-94-015-8048-9

Hydraulic Formula Collection 2018. (2019). Edited by Hydraulic Engineering Committee. *Hydraulic Formula Collection Editorial Subcommittee*, JSCE, ISBN 978-4-8106-0835-9, 927 pages, March.

Japan Rivers Association. (2005). *Revised Explanation, River management facility structure order.* National Institute for Land and Infrastructure Development (ed.), Revised 20th Edition, Gihodo Shuppan.

KENEK CO.. LDT official website. Retrieved October 16, 2023, from https://www.kenek-co.com/english/index.html

Kim, S., Salmasi, F., Ghorbani, M. A., Karimi, V., Malik, A., & Kahya, E. (2017). *Energy Dissipation in Rough Chute: Experimental Approach Versus Artificial Intelligence Modeling*, Chapter 12. Springer Nature Singapore, pp. 227-247. https://doi.org/10.1007/978-981-15-5772-9_12

Liu, M., Rajaratnam, N., & Zhu, D. Z. (2004). Turbulence structure of hydraulic jumps of low Froude numbers. *Journal of Hydraulic Engineering, 130*(6), 511-520. https://doi.org/10.1061/(ASCE)0733-9429(2004)130:6(511)

Ohtsu, I., & Takahashi, M. (2012). Aerated flow characteristics of skimming flow over stepped chutes. *Journal of Hydraulic Research, 50*(4), 427-434. https://doi.org/10.1080/00221686.2012.702859

Pagliara, S., & Palermo, M. (2015). Hydraulic jumps on rough and smooth beds: aggregate approach for

horizontal and adverse-sloped beds. *Journal of Hydraulic Research, 53*(2), 243-252. https://doi.org/10.1080/00221686.2015.1017778

Pagliara, S., Lotti, I., & Palermo, M. (2008). Hydraulic Jump on Rough Bed of Stream Rehabilitation Structures. *Journal of Hydro-environment Research, 2,* 29-38. https://doi.org/10.1016/j.jher.2008.06.001

Pagliara, S., Radecki-Pawlik, A., Palermo, M., & Plesiński, K. (2017). Block ramps in curved rivers: morphology analysis and prototype data supported design criteria for mild bed slopes. *River Research and Applications, 33*(3), 1-28. https://doi.org/10.1002/rra.3083

Takashi, I., Kurakami, Y., Sanagawa, T., & Nihei, Y. (2021). Experimental study on reduction of local scour due to various scour protection around Pier. *Journal of JSCE Proceedings B1 (Hydraulic Engineering), 77*, 763-768. (in Japanese) https://doi.org/10.2208/jscejhe.77.2_I_763

Umeda, S., Yamazaki, T., & Yuhi, M. (2010). Effects of foundation location on scour process around a cylindrical bridge pier. *Journal of JSCE Proceedings B1 (Hydraulic Engineering), 54*, 835-840. (in Japanese)

Vijayasree, B. A., Eldho, T. I., Mazumder, B. S., & Ahmad, N. (2019). Influence of bridge pier shape on flow field and scour geometry. *International Journal of River Basin Management*, *17*(1), 109-129. https://doi.org/10.1080/15715124.2017.1394315

Yasuda, Y. (2016). Contribution due to river engineering in preservation for diadromous aquatic animals. *Aqua, 38*, 387-396. (in Japanese)

Yasuda, Y., & Fuchino, N. (2022). *The Efficacy of Artificially Assembled Boulder Installations in Improving Migration Routes for Aquatic Animals*. River Basin Management Under a Changing, Intech Open, United kingdom, pp. 1-20. https://doi.org/10.5772/intechopen.105198

Yasuda, Y., & Ishitsuka, T. (2023). Experimental Investigation on Countermeasures for Gravel Bed Scouring and Driftwood Deposition around Pier. *Journal of Environmental Science Studies, 6*(2), 26-37. https://doi.org/10.20849/jess.v6i2.1395

Yasuda, Y., & Shinozaki, R. (2018). The Effect of Drop Shape on Velocity Characteristics in Hydraulic Jump below Drop Structures. *Journal of Japan Society of Civil Engineers, Ser. B1 (Hydraulic engineering), 74*(5), I_727-I_732. (in Japanese). https://doi.org/10.2208/jscejhe.74.5_I_727

Yasuda, Y., & Shinozaki, R. (2019). Experimental Investigation of Velocity Characteristics in Plunging Flow below Low Drop Structures. *Journal of Japan Society of Civil Engineers, Ser. B1 (Hydraulic engineering), 75*(2), I_805-I_810. (in Japanese). https://doi.org/10.2208/jscejhe.75.2_I_805

Yasuda, Y., & Suzuki, S. (2023). Prevention Due to Assembled Boulders Against Local Scouring in Low-head Hydraulic Structures. *Journal of Environmental Science Studies, 6*(2), 38-50. https://doi.org/10.20849/jess.v6i2.1397

Yasuda, Y., & Uemura, M. (2023). Experimental Investigation on Velocity Fields of Seepage Flow Inside Gravel Mount. *Journal of Environmental Science Studies, 6*(2), 14-25. https://doi.org/10.20849/jess.v6i2.1373

Yasuda, Y., & Wang, J. (2024). Countermeasure of Protection against Local Scouring Downstream of Concrete Check Dams. *Journal of Environmental Science Studies, 7*(1), 10-20. https://doi.org/10.20849/jess.v7i1.1433

Yasuda, Y., Yasuda, K., & Beretta Piccoli, P. (2023). *River Improvement*, Chapter 22, Eel Science. *The Japanese Society of Fisheries Science 2023*, Springer, Singapore, pp. 293-303. https://doi.org/10.1007/978-981-99-5692-0_22

Zhang, Z. (2022). Study on local scour protection countermeasures of bridge pier. *Highlights in Science, Engineering and Technology, AGECT, 28*, 464-470. https://doi.org/10.54097/hset.v28i.4878